

A Salinity Module for SWAT to Simulate Salt Ion Fate and Transport at the Watershed Scale

Ryan T. Bailey^{1*}, Saman Tavakoli-Kivi¹, Xiaolu Wei¹

¹ Department of Civil and Environmental Engineering, Colorado State University, 1372 Campus Delivery, Fort Collins, CO, 80523-1372, United States.

*Correspondence to: Ryan Bailey (rtbailey@colostate.edu)

Abstract. Salinity is one of the most common water quality threats in river basins and irrigated regions worldwide. However, no available numerical models simulate all major processes affecting salt ion fate and transport at the watershed scale. This study presents a new salinity module for the SWAT model that simulates the fate and transport of 8 major salt ions (SO_4 , Ca , Mg , SO_4^{2-} , Ca^{2+} , Mg^{2+} , Na^+ , K^+ , Cl , CO_3^{2-} , CO_3^{2-} , HCO_3^-) in a watershed system. The module accounts for salt transport in surface runoff, soil percolation, lateral flow, groundwater, and streams, and equilibrium chemistry reactions in soil layers and the aquifer. The module consists of several new subroutines that are imbedded within the SWAT modelling code and one input file containing soil salinity and aquifer salinity data for the watershed. The model is applied to a 732 km² salinity-impaired irrigated region within the Arkansas River Valley in southeastern Colorado, and tested against root zone soil salinity, groundwater salt ion concentration, groundwater salt loadings to the river network, and in-stream salt ion concentration. The model can be a useful tool in simulating baseline salinity transport and investigating salinity best management practices in watersheds of varying spatial scales worldwide.

1 Introduction

Salinity is one of the most common water quality threats in river basins and irrigated regions worldwide. Sustainability of crop production in irrigated areas in semi-arid and arid areas is threatened by over-irrigation, poor quality of irrigation water (high salinity), inadequate drainage, shallow saline groundwater, and salinization of soil and underlying groundwater, all of which can lead to decreasing crop yield. Of the estimated 260 million ha of irrigated land worldwide, approximately 20-30 million ha (7-12%) is salinized (Tanji and Kielen, 2002), with a loss of 0.25 to 0.5 million ha each year globally. Approximately 8.8 million ha in western Australia alone may be lost to production by the year 2050 (NLWRA, 2001), and 25% of the Indus River basin is affected by high salinity. Within the western United States, 27-28% of irrigated land has experienced sharp declines in crop productivity due to high salinity (Umali, 1993; Tanji and Kielen, 2002), thereby rendering irrigated-induced salinity as the principal water quality problem in the semi-arid regions of the western United States.

Salinization of soil and groundwater systems is caused by both natural processes and human-made activities. Salt naturally can be dissolved from parent rock and soil material, with salt minerals (e.g. gypsum CaSO_4 , halite NaCl) dissolving to mobile ions such as Ca^{2+} , SO_4^{2-} , Na^+ , and Cl^- . In addition, salt ions can accumulate in the shallow soil zone due to waterlogging, which is a result of over-irrigating and irrigating in areas with inadequate drainage. Salts moving up into the soil zone can become evapo-concentrated due to the removal of pure water by crop roots. Soil water salinization leads to a decrease in osmotic potential, i.e. the potential for water to move from soil to the crop root cells via osmosis, leading to a decrease in crop production.

39 Numerical models have been used extensively to assess saline conditions, simulate salt movement across landscapes and
40 within soil profiles, predict salt build-up and movement in the root zone, and investigate the impact of best management
41 practices (Oosterbaan, 2005; Schoups et al., 2005; Burkhalter and Gates, 2006; Singh and Panda, 2012). Available models that
42 either have inherent salinity modules or can be applied to salinity transport problems include UNSATCHEM (Šimůnek and
43 Suarez, 1994), HYDRUS linked with UNSATCHEM (Šimůnek et al., 2012); DRAINMOD, LEACHC (Wagenet and Hutson,
44 1987), SAHYSMOD (Oosterbaan, 2005; Singh and Panda, 2012), CATSALT, and MT3DMS (Burkhalter and Gates, 2006).

45 Whereas several of these models include major ion chemistry for salt ions (e.g. precipitation-dissolution, cation exchange,
46 complexation) (UNSATCHEM, HYDRUS), their application typically is limited to small field-scale or soil-profile domains (e.g.
47 Kaledhonkar and Keshari, 2006; Schoups et al., 2006; Kaledhonkar et al., 2012; Rasouli et al., 2013). Conversely, models such
48 as SAHYSMOD and MT3DMS have been applied to regional-scale problems, but lack the reaction chemistry and treat salinity
49 as a conservative solute. SAHYSMOD uses seasonal water and salt balance components for large-scale systems on a seasonal
50 time step (Singh and Panda, 2012). MT3DMS is a finite-difference contaminant transport groundwater model that uses
51 MODFLOW output for groundwater flow rates, but does not include salt ion solution chemistry (Burkhalter and Gates, 2006).
52 Schoups et al. (2005) used a hydro-salinity model that couples MODHMS with UNSATCHEM to simulate subsurface salt
53 transport and storage in a 1,400,140 km² region of the San Joaquin Valley, California. The model, however, does not consider
54 salinity transport in surface runoff or salt transport in streams, limiting results to soil salinity and groundwater. Currently, there is
55 no model that simulates salt transport in all major hydrologic pathways (surface runoff, soil percolation and leaching,
56 groundwater flow, streamflow) at the watershed-scale that also considers important solution reaction chemistry. Such a model is
57 important for assessing watershed-scale and basin-scale salt movement and investigating the impact of large-scale salinity
58 remediation schemes.

59 The objective of this paper is to present a salinity transport modeling code that can be used to simulate the fate and transport
60 of the major ions (~~SO₄, Ca, Mg, SO₄²⁻, Ca²⁺, Mg²⁺, Na⁺, K⁺, Cl, CO₃²⁻, CO₃²⁻, HCO₃⁻~~) in a watershed hydrologic system. The
61 salinity module is implemented within the SWAT modeling code, and thereby salt transport pathways include surface runoff,
62 percolation, soil ~~later~~lateral flow, groundwater flow and streamflow. The soil water and groundwater concentration of each salt
63 ion is also affected by equilibrium chemistry reactions: precipitation-dissolution, complexation, and cation exchange. The use of
64 the model is demonstrated through application to a 732 km² region of the Lower Arkansas River Valley (LARV) in southeastern
65 Colorado, an irrigated alluvial valley in which soil and groundwater salinization has occurred over the past few decades. The
66 model is tested against salt ion and total dissolved solids (TDS) concentration in surface water (Arkansas River and its
67 tributaries), groundwater (from a network of monitoring wells), and soil water (from a large dataset of soil salinity
68 measurements). The salinity module for SWAT can be applied to any watershed to simulate baseline conditions and to test the
69 effect of best management practices on watershed salinity.

71 **2 Development of the SWAT Salinity Module**

72 This section provides a brief overview of the SWAT model, followed by a description of the SWAT salinity module. Sect. 3
73 demonstrates the use of the salinity module to a regional-scale irrigated stream-aquifer system in the Lower Arkansas River
74 Valley, Colorado.

75 **2.1 The SWAT Model**

76 The SWAT (Soil and Water Assessment Tool, Arnold et al., 1998) hydrologic model simulates water flow, nutrient mass
77 transport and sediment mass transport at the watershed scale. It is a continuous, daily time-step, basin-scale, distributed-

Formatted: Indent: First line: 0.25"

parameter watershed model that simulates water flow and nutrient (nitrogen, phosphorus) transport in surface runoff, soil percolation, soil ~~later~~lateral flow, groundwater flow and discharge to streams, and streamflow. The watershed is divided into subbasins, which are then further divided into multiple unique combinations (Hydrologic Response Units HRUs) of land use, soil type and topographic slope for which detailed water and nutrient mass balance calculations are performed. Routing algorithms route water and nutrient mass through the stream network to the watershed outlet. SWAT has been applied to hundreds of watersheds and river basins worldwide to assess water supply and nutrient contamination under baseline conditions (Abbaspour et al., 2015) and scenarios of land use change (Zhao et al., 2016; Zuo et al., 2016; Napoli et al., 2017), best management practices (Arabi et al., 2006; Maringanti et al., 2009; Ullrich and Volk, 2009; Dechmi and Skhiri, 2013), and climate change (Jyrkama and Sykes, 2007; Ficklin et al., 2009; Tweed et al., 2009; Haddeland et al., 2010; Brown et al., 2015). However, it has not yet been applied to salinity issues.

2.2 Salinity Module for SWAT

The new SWAT salinity module ~~simulates~~allows SWAT to simulate the fate and transport of 8 major salt ions (SO_4 , ~~Ca~~, Mg , SO_4^{2-} , Ca^{2+} , Mg^{2+} , Na^+ , K^+ , Cl^- , CO_3^{2-} , CO_3^{2-} , HCO_3^-) via surface runoff, soil ~~later~~lateral flow, soil percolation and leaching, groundwater flow, and streamflow, subject to chemical reactions such as precipitation-dissolution, complexation, and cation exchange within soil layers and the alluvial aquifer. The module also simulates the loading of salt mass to the soil profile via saline irrigation water from both surface water (subbasin channel) and groundwater (aquifer) sources. A watershed cross-section schematic describing these processes is shown in Figure 1.

The salinity module is implemented directly into the SWAT ~~modelling code (FORTRAN code)~~, with new subroutines developed for salt chemistry (*salt_chem*), salt irrigation loading (*salt_irrig*), salinity percolation and leaching (*salt_lch*), and salt groundwater transport and loading to streams (*salt_gw*). Other standard SWAT subroutines are modified to incorporate salt ion transport and effects, such as ~~SWAT's crop growth modules~~, lagging solutes in surface runoff and groundwater flow (*surfstor*, *substor*), and routing solutes through the stream network (*watqual*). These subroutines are shown in Figure 2 within the general SWAT modeling code data flow. For each day loop, the mass balance calculations for each HRU are performed. Salt subroutines are shown for chemical equilibrium, irrigation loading, salt leaching, soil salinity stress, salt groundwater transport and loading, and lagging in surface runoff and groundwater flow. At the end of the HRU calculations, the water, sediment, nutrients, and salt ~~ion~~ mass is routed through the stream network, with in-stream concentration of each salt ion simulated for each SWAT subbasin. Details for each salt ion process are now presented. For the equations presented, S refers to salt mass, and the subscript i refers to the 8 major ions. For the transport equations, calculations are similar to SWAT's transport equations for nitrate. Salinity module input data and output data also will be discussed later in this section.

2.2.1 Salt in Surface Runoff ("*salt_lch*" and "*surfstor*" subroutines)

The mass of each salt ion can be transferred from an HRU to the subbasin channel via surface runoff. The salt ion mass generated in surface runoff: $S'_{i,surf}$ ($S'_{i,surf}$) (kg/ha) for the current day is calculated as:

$$S'_{i,surf} = \beta_{S_i} \cdot C_{S_i} \cdot Q_{surf} \quad (1)$$

where β_{S_i} is the salinity percolation coefficient, C_{S_i} is the concentration of the i^{th} salt ion in the mobile water for the top 10 mm of soil (kg salt /mm water), and Q_{surf} is the surface water generated from the HRU on a given day (mm water). As only a portion of the surface runoff and lateral flow reaches the subbasin channel on the day it is generated, SWAT uses a storage feature to surface runoff. The salt ion mass reaching the subbasin channel on the current day via surface runoff is calculated as:

Formatted: Font: Italic

Formatted: Font: Italic

Formatted: Font: Italic

115
$$S'_{i,surf} = (S'_{i,surf} + S_{i,surfstor}) \cdot \left(1 - \exp\left[\frac{-surlag}{t_{conc}}\right] \right) \quad (2)$$

116 where $S_{i,surf}$ is the mass of the i^{th} salt ion that reaches the subbasin channel on the current day (kg/ha), $S_{i,surfstor}$ is the salt ion
 117 surface runoff stored or lagged from the previous day (kg/ha), $surlag$ is the surface runoff lag coefficient, and t_{conc} is the time of
 118 concentration for the HRU (hrs).

121 **2.2.2 Salt in Lateral Flow (“*salt_lch*” and “*substor*”- subroutines)**

122 The salt ion mass generated in lateral flow $S'_{i,lat,ly}$ (kg/ha) from a soil layer for the current day is calculated as:

123
$$S'_{i,lat,ly} = C_{S_i} \cdot Q_{lat,ly} \quad (3)$$

124 where $Q_{lat,ly}$ is the water discharge from the layer by lateral flow (mm water). Similar to surface runoff, only a portion of the
 125 lateral flow will reach the subbasin channel on the day it is generated, and thus the salt ion mass reaching the channel on the
 126 current day $S_{i,lat,ly}$ (kg/ha) via lateral flow is calculated as:

127
$$S_{i,lat,ly} = (S'_{i,lat,ly} + S_{i,latstor}) \cdot \left(1 - \exp\left[\frac{-1}{TT_{lat}}\right] \right) \quad (4)$$

128 where $S_{i,latstor}$ is the salt ion mass stored or lagged from the previous day (kg/ha) and TT_{lat} is the lateral flow travel time
 129 (days).

130 **2.2.3 Salt in Soil Percolation (“*salt_lch*” subroutine)**

131 The salinity module tracks the mass of each salt ion (kg/ha) in each soil layer. The salt ion mass moved to the underlying
 132 soil layer by percolation $S_{i,perc,ly}$ (kg/ha) is calculated as:

133
$$S_{i,perc,ly} = C_{S_i} \cdot Q_{perc,ly} \quad (5)$$

134 where $Q_{perc,ly}$ is the amount of water percolating to the underlying soil layer on a given day (mm water). After percolation has
 135 been simulated, the concentration of each salt ion (mg/L) in each soil layer is calculated using the area (m²) of the HRU and the
 136 volume of water in the soil layer (m³). The leached salt ion mass is added to the shallow aquifer using the following:

137
$$S_{i,rech} = \left[(1 - gw_{delay}) \cdot S_{i,perc} \right] + (gw_{delay} \cdot S_{i,rech,t-1}) \quad (6)$$

138 where $S_{i,rech}$ is the salt ion mass loaded to the water table via recharge (kg/ha), $S_{i,perc}$ is the salt ion mass percolated from the
 139 bottom layer of the soil profile, $S_{i,rech,t-1}$ is the leached salt ion ~~mass~~ from the previous day, and gw_{delay} is the groundwater
 140 delay time, i.e. the time required for water leaving the bottom of the root zone to reach the water table (days).

141 **2.2.4 Salt in Groundwater Flow (“*salt_gw*” subroutine)**

142 The salinity module tracks the mass of each salt ion (kg/ha) in the aquifer. The salt ion mass generated in groundwater flow
 143 $S'_{i,gw}$ (kg/ha) from the aquifer for the current day is calculated as:

144
$$S'_{i,gw} = C_{S_i} \cdot Q_{gw} \quad (7)$$

Formatted: Font: Italic

Formatted: Font: Italic

Formatted: Font: Italic

Formatted: Font: Italic

145 where $C_{S_{gw}}$ is the salt ion concentration in the aquifer (kg salt /mm water), and Q_{gw} is the groundwater flow generated for the HRU
146 for the current day (mm water). The concentration of each salt ion in each HRU aquifer is calculated on each day by dividing the
147 total mass of the salt ion (g) by the total volume of groundwater (m^3).

148 **2.2.5 Salt in Streamflow (“*watqual*” subroutine)**

149 Water is routed through the watershed channel network using the variable storage routing method, a variation of the
150 kinematic wave model (Neitsch et al., 2011). The mass of each salt ion is routed through the channel network with water, with no
151 chemical reactions changing in-stream salt ion concentration. Similar to any constituent in SWAT, salt ion loadings (kg/day) can
152 be specified for any subbasin reach of the watershed.

153 **2.2.6 Salt Loading in Irrigation water (“*salt_irrig*” subroutine)**

154 Salt ion mass is added to the soil profile via irrigation water, with water derived from either the aquifer (groundwater
155 pumping) or from surface water diversions. Including constituent mass in irrigation water is a new feature for SWAT, as the
156 original code does not account for nutrient (N, P) mass in irrigation water. If the irrigation water source is a subbasin reach
157 (surface water irrigation), the concentration of each salt ion is multiplied by the volume of applied irrigation water (depth of
158 water * HRU area) to determine the mass of each salt ion (kg/ha) to add to the first soil layer. If the irrigation water source is the
159 shallow aquifer, the concentration of each salt ion in the HRU aquifer is used to estimate salt loading to the first soil layer. The
160 salt ion mass is then removed from the HRU aquifer.

161 **2.2.7 Salt Solution Chemistry**

162 The salinity chemistry implemented into SWAT is based on the Salinity Equilibrium Chemistry (SEC) module developed
163 for soil-aquifer systems (Tavakoli-Kivi, 2018 et al., 2019). The equations for salinity solution chemistry presented here are
164 performed for each HRU soil layer and for each HRU. The solution chemistry in this module is similar to that implemented in
165 other water chemistry models [UNSATCHEM: Šimůnek et al. (2012), PHREEQC: Parkhurst and Appelo (2013), MINTEQA2:
166 Paz-Garcia et al. (2013)]. Thus, only basic details are presented here.

167 The SEC module includes 8 aqueous components, 10 complexed species, five solid (salt mineral) species, and four exchange
168 species (Table 1). The 8 aqueous components (SO_4^{2-} , Ca^{2+} , Mg^{2+} , Na^+ , K^+ , Cl^- , CO_3^{2-} , HCO_3^-) are included
169 due to their presence in the majority of soil-aquifer systems. The five salt minerals ($CaSO_4$, $CaCO_3$, $MgCO_3$, $NaCl$, $MgSO_4$) also
170 are included due to their presence in many soil-aquifer systems, although the module can be amended to include any mineral
171 species. The module simulates the dissolved concentration (mg/L) of the 8 ions in soil water and groundwater and the solid mass
172 concentration of the five salt mineral species in the soil and the aquifer sediment according to precipitation-dissolution,
173 complexation, and cation exchange reactions.

174 For these calculations, the duration of the model time step (daily time step for SWAT) is assumed long enough for all
175 constituent reactions to achieve equilibrium. The concentration of species at equilibrium is calculated using a stoichiometric
176 algorithm approach, in which mass balance and mass action equations are solved simultaneously. This method is used in other
177 water chemical equilibrium packages such as PHREEQC (Parkhurst and Appelo, 2013) and MINTEQA2 (Paz-Garcia et al.,
178 2013).

179 *Law of Mass Action*

180 At equilibrium, the concentration of all reactants and products are related using the equilibrium constant K :

$$181 \quad K = \frac{(C)^c (D)^d}{(A)^a (B)^b} \quad (8)$$

Formatted: Font: Italic

Formatted: Font: Italic

182 | where A and B are reactants, C and D are ~~reactants~~products, a, b, c, and d are constants, and the parentheses denote solute
 183 | activities. The activity of the i^{th} solute, i_A , is computed by multiplying the activity coefficient γ_i by the molal concentration, where
 184 | γ_i depends on the ionic strength I of the solution:

185
$$I = \frac{1}{2} \sum m_i z_i^2 \quad (9)$$

186 | where z_i is the charge number of the i^{th} ion and m_i is the molality (mol/kg H₂O). γ_i is then given as:

187
$$\begin{cases} \log \gamma_i = -\frac{A_a z_i^2 \sqrt{I}}{1 + B_a a_i \sqrt{I}} & I < 0.1 \\ \log \gamma_i = -A z_i^2 \left(\frac{\sqrt{I}}{1 + \sqrt{I}} - 0.3I \right) & 0.1 < I < 0.5 \end{cases} \quad (10)$$

188 | where A_a and B_a are temperature dependent constants ($A_a = 0.5085 \text{ m}^{-1}$ and $B_a = 0.3285 \times 10^{10} \text{ m}^{-1}$ at 25° C) and a_i is a measure of
 189 | effective diameter of a hydrated ion i . The first equation in (10) is the Debye-Huckle equation for dilute solutions, and the second
 190 | equation is the Davis equation.

191 *Mass Balance Equations*

192 | The mass of each element in the system, either in ion or complexed form, is tracked by a set of mass balance equations.

193 | Equations for SO₄, Cl, Ca, and Na are:

194
$$\text{SO}_{4,T} = [\text{SO}_4^{2-}] + [\text{CaSO}_4^0] + [\text{MgSO}_4^0] + [\text{NaSO}_4^-] + [\text{KSO}_4^-] \quad (11a)$$

195
$$\text{Cl}_T = [\text{Cl}^-] \quad (11b)$$

196
$$\text{Ca}_T = [\text{Ca}^{2+}] + [\text{CaSO}_4^0] + [\text{CaCO}_3^0] + [\text{CaHCO}_3^+] \quad (11c)$$

197
$$\text{Na}_T = [\text{Na}^+] + [\text{NaSO}_4^-] + [\text{NaCO}_3^-] + [\text{NaHCO}_3^0] \quad \text{Na}_T = [\text{Na}^+] + [\text{NaSO}_4^-] + [\text{NaCO}_3^0] + [\text{NaHCO}_3^0] \quad (11d)$$

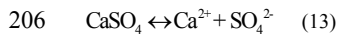
198 | where T denotes total concentration and brackets indicate species' molality. Similar equations are written for Mg, K, CO₃, and
 199 | HCO₃.

200 *Precipitation-Dissolution Reactions*

201 | Salt minerals (AB_s) can dissolve or precipitate according to the stoichiometric reaction



203 | The salt mineral will ~~dissolved~~dissolve if the solution is under-saturated in ~~in~~ regards to A_{aq}^+ and B_{aq}^- , and will
 204 | precipitate if the solution is super-saturated. Salt minerals in the SEC module include CaSO₄, CaCO₃, MgCO₃, MgSO₄, and
 205 | NaCl, due to their common occurrence in aquifers. For example:



207 | with a solubility product constant:

208
$$K_{\text{sp}_{\text{CaSO}_4}} = \frac{(\text{Ca}^{2+})(\text{SO}_4^{2-})}{(\text{CaSO}_4)} \quad (14)$$

209 | Within the SEC module, minerals are added to the system one at a time, with the solubility limits of each mineral used to
 210 | determine the direction of each reaction (precipitation or dissolution).

211 *Complexation Reactions*

Formatted: Font: Italic

Formatted: Font: Italic, Subscript

212 Based on the law of mass action, equilibrium equations are written for all complexed species. For example, the equation for
213 $CaSO_4^0$ is:

$$214 \quad K_{CaSO_4} = \frac{(Ca^{2+})(SO_4^{2-})}{CaSO_4^0} \quad (15)$$

215 where K_{CaSO_4} is the equilibrium constant and is equal to 0.004866. Equations and equilibrium constants for the remaining
216 9 complexed species are shown in Supporting Material.

217 Cation Exchange Reactions

218 Cation exchange is calculated to determine the sorbed and released ions from sediment surfaces to the solution. The order of
219 replaceability is $Na > K > Mg > Ca$, determined by Coulomb's Law. The cation reaction as an equivalent reactions represented
220 by Gapon equation:

$$221 \quad X_{1/mM} + 1/n N^{n+} = X_{1/nN} + 1/m X^{m+} \quad (16)$$

222 where $X_{1/mM}$ is exchangeable cation M on the surface (meq/100g), $X_{1/nN}$ is exchangeable cation N on the surface (meq/100g),
223 M and N are metal cations, and $m+$ and $n+$ are the charges of cations M and N respectively. Using the cation exchange capacity
224 of the soil and a coefficient of Gapon selectivity coefficient for each reaction, concentration of each exchangeable species is
225 determined.

226
227 The salinity chemistry reactions (precipitation-dissolution, complexation, cation exchange) are simulated for each HRU
228 within the *salt_chem* subroutine (see Figure 2). Within this subroutine, the chemistry reactions are applied to the current
229 simulated concentration values of the 5 salt minerals and the 8 salt ions for each soil layer and aquifer, to calculate new
230 concentration values. These new concentration values are then used to simulate salt leaching (*salt_lch* subroutine) and salt ion
231 loading in surface runoff (*surfstor*) and groundwater flow (*salt_gw_substor*) (Figure 2). At the end of each daily time step, the
232 simulated salt ion mass (kg) in each transport pathway (irrigation, leaching, runoff, percolation, lateral flow, groundwater flow,
233 dissolution/precipitation) is stored for mass balance assessment and output.

235 2.2.8 Salinity Module Input/Output

236 Required data for running the SWAT salinity module include: precipitation-dissolution solubility products for the five salt
237 minerals ($CaSO_4$, $CaCO_3$, $MgCO_3$, $NaCl$, $MgSO_4$), initial concentration of salt ions in soil water and groundwater, and initial salt
238 mineral solid concentration (% of bulk soil) in soil and aquifer sediment. Initial concentrations are required for each HRU.
239 However, as will be shown in Sect. 3.3.2.4, using uniform (i.e. at each HRU values are given the same value) concentration
240 values yields the same result as using spatially-variable initial concentrations, if a warm-up period of several years is used in the
241 SWAT simulation.

242 All input data are provided in a single input file, "*salt_input*". To turn on the salinity module, a single line has been
243 added at the end of the *file.cio* file, with a flag (0 or 1) being read (0 or 1) to exclude/include the salinity module. If the flag is
244 set to 1, the SWAT code will open and read the contents of the *salt_input* file.

245 Four output files contain simulated salt ion data for the watershed (Figure 2):

- 246 • *salt_output.std* contains the total salt mass (TDS) transported via lateral flow, groundwater flow, surface runoff, tile
247 drains, percolation, irrigation of surface water, irrigation of groundwater, upflux water, and dissolution, normalized
248 to the area of the watershed (kg/ha).

- salt.output.rch contains loading (kg) and concentration (mg/L) of each salt ion for each subbasin channel, for each day of the simulation. Results from this file can be used to plot time series of salt ion concentration, as shown in Sections 3.3.2.1.
- salt.output.sub contains the total salt mass (TDS) transported via lateral flow, groundwater flow, surface runoff, tile drains, percolation, irrigation of surface water, irrigation of groundwater, and dissolution for each subbasin, for each day of the simulation. The salt loads (kg/ha) are normalized to the subbasin area.
- salt.output.hru contains salt ion concentration in the soil water and in the groundwater for each HRU, for days specified in the salt_input file.

Formatted: List Paragraph, Add space between paragraphs of the same style, Bulleted + Level: 1 + Aligned at: 0.5" + Indent at: 0.75"

Formatted: Font: Times New Roman, Italic, Font color: Text 1

Formatted: Font: Bold

3 Application of SWAT Salinity Module to an Irrigated Stream-Aquifer System

3.1 Study Region: Lower Arkansas River Valley, Colorado

The salinity module is tested for a 732 km² irrigated stream-aquifer system along the Arkansas River in southeastern Colorado (Figure 3A). The region consists the Arkansas River and tributaries (e.g. Timpas Creek, Crooked Arroyo, see Figure 3A) running through and over a thin (~10-15 km in width) and shallow (~10-20 m) sandy alluvial aquifer. The climate is semi-arid, requiring irrigation to supplement rainfall for crop growth. Irrigation water is derived either from the Arkansas River via a system of irrigation canals or from the aquifer via a network of ~500 pumping wells (Figure 3A). Cultivation and associated irrigation occurs March through November.

Salinization of soil, groundwater, and surface water in the region has steadily worsened since the 1970s due to increased irrigation diversions from the Arkansas River, high water tables due to excessive water applications to fields, and the existence of salt minerals, particularly gypsum (CaSO₄) (Konikow and Person, 1985; Goff et al., 1998; Gates et al., 2002; Gates et al., 2016). Soil salinity levels under about 70% of the area exceed threshold tolerance for crops, with the regional average of crop yield reduction from salinity and waterlogging estimated to range from 11 to 19% (Gates et al., 2002; Morway and Gates, 2012).

From sampling groundwater from a network of 82 observation wells (see Figure 3B) (sampling from June 2006 to May 2010), average salinity concentration of shallow groundwater is approximately ~~2,700~~~~2700~~ to ~~3,000~~~~3000~~ mg/L, and annual salt loading to the Arkansas River from groundwater return flows is about 500 kg per irrigated ha, per km of the river. In the 1990s, 68% of producers stated that high salinity levels are a significant concern (Fraser et al., 1999). For the region modeled in this study, average TDS concentration ($\overline{C_{TDS}}$ C_{TDS}) in groundwater is ~~3,334~~~~3334~~ mg/L (443 samples), with a minimum of 459 mg/L

and a maximum of ~~44,600~~~~44600~~ mg/L. The presence of gypsum is revealed in the high concentration of SO₄ ($\overline{C_{SO_4}}$ C_{SO_4}), with average, minimum, and maximum concentrations of ~~1,878~~~~1878~~ mg/L, 147 mg/L, and ~~29,457~~~~29457~~ mg/L, respectively. Average soil water salinity, ~~using based on~~ electrical conductivity (~~EC of a soil paste extract~~ (EC_e), is 4.11 dS/m (~~54,700~~~~54700~~ measurements), with minimum and maximum of 0.9 dS/m and 56.5 dS/m, respectively (~~Morway and Gates, 2012~~). ~~These values were estimated from measurements of apparent bulk soil conductivity, taken with a Geonics EM-38 electromagnetic induction sensor, as described in Morway and Gates (2012). Surveys were performed during the months of March-September for 1999-2005.~~ Based on 6 surface water sampling sites (4 in the Arkansas River, 2 in tributaries; Figure 3B), average $\overline{C_{TDS}}$ C_{TDS} and $\overline{C_{SO_4}}$ C_{SO_4} is 1145 mg/L and 560 mg/L, respectively. More details of observed groundwater, soil water, and surface water concentrations are provided in Sect. 3.3.2 when model results are presented.

Formatted: Subscript

3.2 SWAT Model

A previously calibrated and tested SWAT model for the study region is used to simulate salt fate and transport using the developed salinity module. The SWAT model is detailed in Wei et al. (2018). The region was divided into 72 subbasins (see Figure 3B). [The digital elevation model \(DEM\), stream network, soil map, land-use map, climate data, streamflow, and canal diversion data were obtained from the USGS, NRCS, and several state agencies, as summarized in Wei et al. \(2018\).](#) A method was developed to apply SWAT to highly-managed irrigated watersheds, and included: designating each cultivated field as an individual HRU (see Figure 3B for the map of fields); crop rotations to simulate the effects of changing crop types for each field during the 11-year simulation; seepage to the aquifer from the earthen irrigation canals; and SWAT's auto-irrigation algorithms to trigger irrigation events based on plant water demand for both surface water irrigation and groundwater irrigation. The method resulted in 5,270,5270 HRUs. Implementing canal seepage required a slight change to the SWAT modeling code to add pre-processed, estimated canal seepage to [the](#) HRU aquifer. Canal seepage rates were obtained from field measurements (Susfalk ~~et al.~~, 2008; Martin et al., 2014).

The model was run for the 1999-2009 time period, with simulated streamflow compared to observed hydrographs at 5 stream gages (Rocky Ford, La Junta, Las Animas, Timpas Creek, Crooked Arroyo; see Figure 3B) for model testing (Wei et al., 2018). [Calibration was performed using SWAT-CUP \(Abbaspour et al., 2008\) using the observed streamflow at the Rocky Ford, Las Animas, and Timpas Creek stations. Twenty parameters were targeted for modification during the calibration process, with the following exhibiting strong control on streamflow: SCS runoff curve number, Manning's \$n\$ value for the main channel, effective hydraulic conductivity of the channel, initial volume of groundwater, recharge delay time, fraction of deep aquifer percolation, and snowfall temperature. Further details regarding calibration, model implementation, and hydrologic results are found in Wei et al. \(2018\).](#)

3.3 SWAT Model with Salinity Module

3.3.1 Model Construction and Simulation

The SWAT model [with the new salinity module](#) is run from April 1 1999 to December 13 2009, with observed data for testing available from June 2006 to December 2009. The 1999-2005 period thus serves as a warm-up simulation period. The calibration period is 2006-2007, and the testing period from 2008-2009. Required inputs include initial soil water and groundwater ion concentrations, initial soil and aquifer sediment salt mineral fractions and, due to the study region being a part of the larger Lower Arkansas River Valley, ion mass loading in the Arkansas River at the upstream end of the modeled region (Catlin Dam; see Figure 3B).

Salt ion mass loading (kg/day) in the Arkansas River at Catlin Dam were estimated using daily measured values of EC (dS/m) and streamflow (m^3/s) and periodic measurements of salt ion concentration (mg/L). Linear relationships were established between EC and the concentration of each salt ion, with this relationship then used to estimate salt ion concentration for each day of the simulation period. The daily in-stream mass of each salt ion was then calculated by multiplying daily salt ion concentration by streamflow, and added to the point-source SWAT input file for the appropriate subbasin. Figure 4A shows the daily loading (kg/day) for each salt ion using this method. The make-up of total mass loading by salt ion is shown in Figure 4B, with SO_4 accounting for 47% of total in-stream salt mass. The linear relationship between EC and selected salt ions (SO_4 , Cl, Na) and TDS is shown in the charts along the bottom of Figure 4. For TDS the R^2 value of the relationship is approximately 0.93.

Initial salt ion concentrations in soil water and groundwater were based on averages of observed groundwater concentrations. For the baseline simulation, the same values were assigned to each HRU. These are 1875 mg/L, 330 mg/L, 175 mg/L, 440 mg/L, 10 mg/L, 150 mg/L, 5 mg/L, and 350 mg/L for C_{SO_4} , C_{Ca} , C_{Mg} , C_{Na} , C_K , C_{Cl} , C_{CO_3} , and C_{HCO_3} ,

324 respectively. The effect of using spatially-varying initial concentrations is explored in additional scenarios. Salt mineral fractions
325 for CaSO₄ and CaCO₃ in the HRU soil layers are based on a soil survey of the region from the Natural Resources Conservation
326 Service (NRCS). The fraction of soil that is CaSO₄ and CaCO₃ was set to 0.1 and 0.01, ~~with all others set to 0.0~~. For the aquifer
327 sediment, fractions are based on the spatial patterns determined in Tavakoli-Kivi ~~(2018)~~ et al. (2019) for a salinity groundwater
328 transport study of the same region. Solubility products for precipitation-dissolution of salt minerals were obtained from literature
329 and from Tavakoli-Kivi ~~(2018)~~ et al. (2019) and are 3.07 x 10⁻⁹, 4.8 x 10⁻⁶, 4.9 x 10⁻⁵, 0.0072, and 37.3 for CaCO₃, MgCO₃,
330 CaSO₄, MgSO₄, and NaCl, respectively, for both soil and aquifer sediments.

331 ~~Only minimal manual~~ Manual calibration was applied to the model, to yield correct magnitudes of salt ion concentration in
332 soil water, groundwater, and stream water. ~~Targeted~~ Due to the predominance of SO₄ and Ca among salt ions in the regional
333 system, ~~targeted~~ parameters were the solubility product of CaSO₄ precipitation-dissolution, and the soil fraction of CaSO₄. The
334 solubility ~~product~~ product was increased from 0.000049 to 0.0003, and the soil fraction of CaSO₄ was decreased from 0.01 to
335 0.009. Model results are tested against in-stream concentration of salt ions, soil ~~water EC (dS/m), salinity,~~ groundwater
336 concentration of salt ions, and groundwater salt ion mass loading to the Arkansas River. ~~Observed soil EC values were obtained~~
337 ~~using a saturated paste extract, and hence comparison with model results will not be as rigorous as for groundwater and surface~~
338 ~~water data. For soil salinity, model results are compared with the 54700 EC_e values from the field survey. EC_e of the soil water in~~
339 ~~the SWAT model layers for each day of the simulation is estimated using the following steps: 1) soil water TDS is computed by~~
340 ~~summing up salt ion concentrations in the soil water; 2) soil water EC (EC_w) is computed by dividing soil water TDS by a TDS~~
341 ~~→ EC_w (dS/m) conversion of 1020 (mg/L per dS/m) based on soil water samples; and 3) EC_e is computed by multiplying EC_w~~
342 ~~by the ratio of stored water (mm) to water at saturation (mm) for the SWAT soil layer. Simulated EC_e values are included in the~~
343 ~~comparison with field-measured EC_e values if the simulated water content of the HRU soil layer is greater than 0.07, since~~
344 ~~Morway and Gates (2012) measured field EC_e only if the soil water content was above this value due to EM-38 sensors being~~
345 ~~unreliable at low water contents (Rhoades et al., 1999).~~

346 Several variations of the model were run to test the effect of 1) initial salt ion concentrations in the HRU soil layers and 2)
347 specified loading of salt ion mass at the upstream end of the Arkansas River. For 1), the variations include uniform initial
348 concentrations (baseline model), random spatially-variable concentrations, and initial concentrations equal to 0. For 2), the
349 variation included one simulation with no loading.

3.3.2 Model Results

351 ~~Model results consist of in-stream salt ion and TDS concentration, hydrologic pathway (groundwater discharge, surface~~
352 ~~runoff, percolation) salt loadings, groundwater salt ion concentration, soil water EC, watershed-wide salt balance, and~~
353 ~~groundwater salt loading to the Arkansas River.~~

3.3.2.1 In-Stream Salt Ion Concentration

354 Simulated and observed in-stream salt ion concentrations (mg/L) are shown in Figure 5 for the Rocky Ford site (Figure 5A),
355 Timpas Creek, Crooked Arroyo, and the Crooked Arroyo site (Figure 5B). Results are shown Las Animas sites for SO₄ each of the
356 8 ions. Overall, the model tracks the measured concentrations well, particularly for SO₄, Ca, Cl, and HCO₃, with the calculated
357 Nash-Sutcliffe model efficiency coefficient (NSE) shown on each plot. Results for TDS at all 5 gaging stations are shown in
358 Figure 6. As can be seen by the trends in concentration and also the NSE values, the SWAT model performs well in replicating
359 in-stream salt ion concentrations, particularly for SO₄ (NSE = 0.60), Ca (NSE = 0.54), HCO₃ (NSE = 0.73), and TDS (NSE =
360 0.69) in the, including the Nash-Sutcliffe model efficiency coefficient (NSE) for each site. NSE values are good for Rocky Ford
361

362 and Crooked Arroyo (0.68 and 0.65), and poor for the other three (< 0.3). However, comparing simulated and measured in-
363 stream concentrations on a daily basis is generally a difficult challenge for watershed modeling.

364 In the two tributaries (Timpas Creek and Crooked Arroyo) and the watershed outlet (Las Animas), the model tends to under-
365 predict the ions of low concentration: Mg, K, Cl, and CO₃. The cause for the under-prediction of these ions may be due to the
366 unobserved presence of MgSO₄, MgCO₃, and NaCl in the soil. These minerals are not observed in NRCS soil surveys of the
367 region, and hence were not included in the baseline model. However, several model scenarios were run to investigate the
368 influence of these minerals. Soil bulk fractions between 0.0001 and 0.0005 were applied for these three minerals, with a large
369 resulting effect on in-stream concentrations of Mg, Na, Cl, and CO₃. For example, using a fraction of 0.0002 resulted in correct
370 magnitude of these four ions at the Las Animas site, but over-estimated concentrations in the tributaries (e.g. Timpas Creek)
371 (Figure 7). This model scenario, however, applied uniform salt mineral fractions of MgSO₄, MgCO₃, and NaCl across all 5270
372 HRUs. Applying spatially-varying fractions across the watershed could provide the correct magnitude of in-stream
373 concentrations of all ions at all stream sampling sites. Regardless, measured in-stream concentrations can provide key
374 information as to the salt minerals present in the watershed, and differences between model output and field data highlight the
375 need for better field survey data of salt mineral content in soils.

376 The in-stream concentrations in the two tributaries (Figure 5B,C) are much more variable than the two sites in the main stem
377 of the Arkansas River at the Rocky Ford gaging site. The model does not perform as well in downstream sites. The two
378 tributaries act as drainage channels for irrigation runoff and groundwater return flows, with NSE at La Junta and at Las Animas
379 equal to 0.34 and 0.25, respectively, although the trends are correct and the magnitudes are correct except for at the downstream-
380 most site (Las Animas), where the model under-predicts total salt concentration. This is also shown by a 1:1 comparison of all
381 salt ion data for the Rocky Ford (Figure 7A) and Las Animas (Figure 7C) sites, which yield R² values of 0.87 and 0.74,
382 respectively. Las Animas also has an R² value of 0.74. However, as the SWAT model often is used to estimate monthly in-
383 stream loads rather than daily in-stream concentration, these results much lower flows than the Arkansas River, and hence the in-
384 stream concentrations are promising regarding the use of SWAT to estimate in-stream salinity affected much more strongly by
385 salt loadings.

386 from irrigation events and associated flow patterns. In regards to the NSE, the model under-performs rather poorly in for the
387 two tributaries (Timpas Creek, Crooked Arroyo), with NSE equal to -0.3229 and 0.4165, respectively, for TDS (Figure 6B, 6C).
388 However, the overall trends and magnitude compare well to observed data. This is shown in the 1:1 plot of all salt ion data for
389 Timpas Creek in Figure 7B8B, resulting in an R² value of 0.7969. The relationship for Crooked Arroyo yields an R² value of
390 0.80- (not shown). This is particularly promising given that there is no specified upstream loading for the tributaries, and hence
391 all salt mass within the stream system is due to surface runoff, lateral flow, and groundwater discharge. Hence, comparing
392 simulated and observed in-stream salinity concentration in these two systems is provides a strong test for the model.

393 Figure 8The summary of in-river salt concentration results is shown by a 1:1 comparison of all salt ion data for the Rocky
394 Ford (Figure 8A) and Las Animas (Figure 8C) sites, which yield R² values of 0.87 and 0.66, respectively. Timpas Creek (Figure
395 8B) has an R² value of 0.69. However, as the SWAT model often is used to estimate monthly in-stream loads rather than daily
396 in-stream concentration, these results are promising regarding the use of SWAT to estimate in-stream salinity loadings.

397 Figure 9 shows the salt loading via the hydrologic pathways of groundwater discharge (Figure 8A9A), surface runoff
398 (8B9B), and percolation from the soil profile to groundwater (8C9C). For Timpas Creek, 96% of salt in the creek water is from
399 groundwater discharge, 3% from surface runoff, and 1% from lateral flow. For Crooked Arroyo, the portions are 91%, 6%, and
400 3%, and for the Arkansas River they are 96%, 3%, and 1%, highlighting the strong influence of groundwater on surface water

401 salt load. This is shown further by examining the domain-wide salt balance, presented in Sect. 3.3.2.3. The mass loading of total
402 salt from the aquifer to the Arkansas River for each day of the 2006-2009 time period is shown in Figure 910. Mass balance plot
403 values are the mean of a stochastic river mass balance calculation of surface water salinity loadings along the length of the
404 Arkansas River within the model domain, using a method similar to Mueller-Price and Gates (2008), with values indicating the
405 mass of salt not accounted for by surface water loadings. These unaccounted for loadings include groundwater, and thus provide
406 an upper limit of in-stream salt loading from groundwater discharge.

409 3.3.2.2 Groundwater and Soil Water Salinity

410 Groundwater salt results are shown by spatial maps and by comparison of frequency distributions. For all simulated results,
411 only concentration values from days on which field samples were taken are included in the analysis. Time-averaged TDS (mg/L),
412 SO₄ (mg/L), and Na (mg/L) in groundwater is shown for each HRU in Figure 4011. Also shown is soil water EC (dS/m) for each
413 HRU soil profile, and the percent of the soil profile (Figure 40E11E) and aquifer (Figure 40F11F) that is CaSO₄ (solid mineral)
414 at the end of the simulation period. These maps are shown to provide an indication of the degree of spatial variation simulated by
415 the salinity-module-model. Variation in each system response is large, with TDS ranging from 0 to ~11,700 mg/L, SO₄ from 0 to
416 ~6700 mg/L, and Na from 0 to ~4,2701270 mg/L. In comparison, if data from an outlier monitoring well are excluded
417 (monitoring well with salinity values more than double of any other monitoring well), the maximum observed values for TDS,
418 SO₄, and Na are 13,00013000 mg/L, 6,5006500 mg/L, and 2,6002600 mg/L.

419 Results for all salt ions are summarized in Table 2. Average concentration of field samples (based on field samples from 82
420 monitoring wells shown in Figure 3B) and HRU-simulated groundwater salinity compares well, particularly for SO₄ (1,8781878
421 mg/L to 2,0582149 mg/L) and for TDS (3,3343334 mg/L to 3,2763508 mg/L). In addition to a comparison of maximum and
422 average values, comparison at various magnitude levels is performed using relative frequency plots, shown in Figure 412.
423 Results for SO₄ (Figure 41A12A), HCO₃ (41B12B), and TDS (41C12C) are shown. Similar to the results shown in Table 2, the
424 comparison for SO₄ and TDS is good, but the model generally under-predicts HCO₃ for most HRUs. A relative frequency plot of
425 observed and simulated EC (dS/m) in the soil profile also is shown (Figure 11D). The average of observed values and simulated
426 values are 4.1 dS/m and 4.8 dS/m, although the majority of observed values are between 2 dS/m and 4 dS/m whereas no such
427 grouping occurs for the simulated values. However, the observed data values are obtained from saturated paste extracts, which
428 therefore lowers the salinity concentration due to the addition of water to bring the soil to saturation. Hence, the "observed"
429 (modified by the saturated paste method) concentrations should be lower than what actual occurs in the field, which may explain
430 the disagreement shown in Figure 11D.

431 A relative frequency plot of observed and simulated EC_e (dS/m) in the soil profile is shown in Figure 12D. The simulated
432 values were taken from HRUs coinciding with cultivated fields for the days of April 15, May 15, June 15, July 15, and August
433 15, for the years 2001-2005. Note that simulated values were taken from each cultivated HRU, whereas the field surveys using
434 the EM-38 sensors were conducted in approximately 100 fields. The average of observed values is 4.1 dS/m, although this
435 number is skewed by extremely high values (> 30 dS/m). If only values < 6.5 dS/m are considered (89% of the samples), then the
436 average is 3.2 dS/m. The average of the simulated values is 2.96 dS/m. As seen from the frequency distribution in Figure 12D,
437 the model tends to under-estimate soil salinity for some of the HRUs, and does not capture the high salinity values (> 7 dS/m).
438 However, the overall magnitude and distribution of values approaches the distribution of the measured values. Note that EM-38

439 measurements have inherent uncertainty. In addition, some of the HRUs included in the analysis are fallow during this period
440 (2002-2005), which may lead to low soil salinity values that were not measured in the field survey.

441 3.3.2.3 Salt Balance

442 The domain-wide salt balance is presented in Figure 42A13A. All salt balance components are included, with all values
443 scaled according to the small salt flux (lateral flow = 1 unit). For the soil profile, salt is added via groundwater irrigation (4217
444 units), surface water irrigation (3329), dissolution of salt minerals (44097), and upflux from the aquifer saturated zone (3944),
445 and removed via percolation (403134), surface runoff (43), and lateral flow (1). A similar salt balance can be performed for each
446 salt ion in the system. Salt removed from the aquifer and added to the soil profile via upflux is approximately 30% of
447 percolation, which compares well to a comparison of water upflux and recharge magnitudes computed by Morway et al. (2013)
448 in a groundwater modeling study of the region using MODFLOW.

449 Of the salt entering the river, 96-797.6% is from groundwater (454162 units out of 456166), and the remaining from surface
450 runoff and lateral flow. Time series of daily loading (kg/ha) for these three components is shown in Figure 42B13B, and loadings
451 for percolation, surface water irrigation, and groundwater irrigation are shown in Figure 42C, showing the seasonal trends in
452 applying irrigation water. These results also 13C, showing the seasonal trends in applying irrigation water. Notice that the highest
453 groundwater loading rates coincide with the “spikes” in the in-stream concentration plots of Figures 5 and 6, indicating the
454 strong influence of groundwater loading on in-stream salt concentrations. The fluctuations in simulated in-stream concentration,
455 however, are larger than observed with the measured values. This is due to the manner in which SWAT simulates groundwater
456 return flow, with a steady-state flow equation for each HRU that provides pulses of groundwater to streams rather than the multi-
457 dimensional groundwater flow equation that provides physically-based, spatially-distributed diffuse flow through the aquifer
458 towards the stream network.

459 Results in Figure 13C indicate that much of the salt leaching from the soil profile is due to dissolution of salt minerals.
460 Results also indicate the importance of including salt mass in applied irrigation water, as it accounts for approximately half of
461 salt leaching to the aquifer. Finally, results show the importance of including precipitation-dissolution in the module, as this
462 process is a large component of the salt balance. Without including this process, the module would severely under-predict salt
463 ion concentrations throughout the watershed, demonstrating the need to include each salt ion individually as opposed to
464 modeling salinity as a conservative solute in the system.

467 3.3.2.4 Scenarios and Model Guidelines

468 The effect of initial salt ion concentrations and upstream salt ion mass loading is summarized by the time series charts in
469 Figure 1314. For the Rocky Ford and Las Animas gaging sites, a time series of simulated SO₄ (mg/L) and TDS (mg/L) is
470 compared for the following scenarios: uniform initial salt ion concentration (“Original”: this refers to the baseline simulation);
471 HRU-variable initial concentration (“Variable IC”); initial concentrations equal to 0 (“Zero IC”); and not accounting for
472 upstream salt ion mass loading at Catlin Dam (“No US Loading”).

473 There are only small differences between using uniform or HRU-variable initial concentrations for soil water and
474 groundwater. Any differences are readily resolved during the warm-up period. Hence, to facilitate model use we recommend that
475 uniform initial concentrations be used.

476 Using initial concentrations equal to 0 mg/L has a significant effect, particularly for downstream sites such as Las Animas
477 (Figure 13C, 14C,D). For this watershed, salt loading to the streams is principally from groundwater, and if soil water and

478 groundwater are not provided with initial salt ion concentrations, the groundwater salt ion loading to subbasin streams is small
479 compared to the baseline simulation. As downstream flow and in-stream salt loading is effected by groundwater loading, these
480 areas (e.g. Las Animas site) experience the effect more acutely than upstream sites such as Rocky Ford (Figure 43A14A,B).
481 However, by the end of the simulation (2009), difference between “Zero IC” and “Original” is small. This is shown by the “Diff”
482 time series for each plot. Therefore, if groundwater discharge is a large component of total water yield for the watershed, “Zero
483 IC” should not be used, or a long warm-up simulation period needs to be used.

484 Not including upstream salt ion loading at Catlin Dam has a stronger effect on the Rocky Ford site (Figure 43A14A,B) than
485 at the outlet (Las Animas) (Figure 43C14C,D). This is due to Las Animas being much farther downstream, and hence there is
486 much more groundwater salt ion loading to the streams that can make up for the salt not included at the upstream end of the
487 Arkansas River at Catlin Dam. Overall, any point sources of in-stream salt should be added, unless only downstream areas are
488 targeted for baseline simulations and best management practice investigation. The effect of neglecting point sources of in-stream
489 salt decreases as the groundwater loading component of total salt yield increases.

490 The importance of including equilibrium chemistry into the salt transport module is demonstrated by the results shown in
491 Figure 4415. The simulated in-stream TDS (mg/L) is shown at the Rocky Ford site (Figure 44A15A), the Timpas Creek site (B),
492 and the Las Animas site (C), for both the original simulation (red line) and a simulation “No SEC” that does not include the SEC
493 module (black line). The “No SEC” simulation therefore represents a system wherein salt is transported through the stream-
494 aquifer system as a conservative species. Clearly, in-stream concentrations are much too low for the simulation without the SEC
495 module. for the Timpas Creek and Las Animas sites. This is due to the neglect of salt mineral dissolution, which in the actual
496 system transfers salt mass from the soil and aquifer material to soil water and groundwater are thereby increases the loading of
497 salt to the stream network. For the Rocky Ford site, the scenarios yield similar results due to the location of the site being close to
498 the upstream end of the modeled region, and thus in-stream concentrations are not affected by groundwater and surface runoff
499 salt loadings to the river. For this system, and likely most watersheds, equilibrium chemistry must be included to establish the
500 correct magnitude of salt loading and concentrations.

501 3.3.3 Model Use and Limitations

502 The salinity module of SWAT differs from other salinity models in that it accounts for salt loading for each major
503 hydrologic pathway in a watershed setting (stream, groundwater, lateral flow, surface runoff, tile drain flow), for each major salt
504 ion, subject to chemical equilibrium reactions (precipitation-dissolution, complexation, cation exchange). As such, it can be used
505 to estimate baseline salt loading within a watershed, and also explore the impact of land management and water management
506 scenarios to mitigate soil salinity, groundwater salinity, and surface water salinity. The model, however, does not simulate
507 physically-based, spatially-distributed groundwater flow and solute transport with an accurate depiction of water table elevation
508 and groundwater head gradient, and thus the trends in groundwater salt loading to streams may not be accurate (see Figure 9). To
509 overcome this issue, the new salinity module could be incorporated into SWAT-MODFLOW (Bailey et al., 2016), which links
510 SWAT and MODFLOW to simulate land surface and subsurface flow processes, and SWAT-MODFLOW-RT3D (Wei et al.,
511 2018), which includes reactive transport of solutes into SWAT-MODFLOW.

513 4 Conclusions

514 This study presents a new watershed-scale salt ion fate and transport model, by developing a salinity module for the SWAT
515 model. The module accounts for salt loading for each major hydrologic pathway in a watershed setting (stream, groundwater,
516 lateral flow, surface runoff, tile drain flow), for each major salt ion (SO₄, Ca, Mg, Na, K, Cl, CO₃, HCO₃). The module also

517 accounts for principal equilibrium chemistry reactions (precipitation-dissolution, complexation, cation exchange). For
518 precipitation-dissolution, five salt minerals (CaSO₄, CaCO₃, MgCO₃, NaCl, MgSO₄) have been included. The model was applied
519 and tested in a 732 km² irrigated stream-aquifer watershed in southeastern Colorado, along the alluvial corridor of the Arkansas
520 River. Model results are tested against in-stream salt ion concentration, groundwater salt ion concentration, soil salinity, and
521 groundwater salt loading to the Arkansas River.

522 The model can be used to assess baseline salinity conditions in a watershed and to explore land and water management
523 strategies aimed at decreasing salinization in river basins. Such strategies may include on-farm management, lining irrigation
524 canals to reduce saline canal seepage, dry-drainage practices, and reducing volumes of applied irrigation water. Due to the
525 simulation of soil water salt ion concentrations and SWAT's simulation of crop growth, the salinity module can also be used to
526 investigate the effect of these strategies on crop yield. Although this study applied the model to an irrigated area, the model can
527 be applied to non-irrigated areas as well.

528

529

530 **Code Availability**

531 The code consists of the original SWAT files, with 6 additional files for the salinity module. All files are *.f FORTRAN files.
532 ~~The code can be~~ The code is available on GitHub (https://github.com/rtbailey8/SWAT_Salinity/). ~~The code can also be made~~
533 available via request from Ryan Bailey at rtbailey@colostate.edu.

534

535 **Author Contribution**

536 Ryan Bailey wrote the salinity module for SWAT and tested the module for the study region. Saman Tavakoli-Kivi prepared the
537 solution chemistry algorithms for the salinity module. Xiaolu Wei prepared and tested the original SWAT model for the study
538 region, and facilitated use of the new salinity module for the constructed SWAT model.

539

540 **Competing Interests**

541 The authors declare that they have no conflict of interest.

542

543 **References**

544 [Abbaspour, K.C., Yang, J., Reichert, P., Vejdani, M., Haghghat, S., and R. Srinivasan \(2008\), SWAT-CUP: SWAT calibration](#)
545 [and uncertainty programs. Zurich, Switzerland: Swiss Federal Institute of Aquatic Science and Technology.](#)

546 Abbaspour, K.C., Rouholahnejad, E., Vaghefi, S., Srinivasan, R., Yang, H., and B. Klove (2015), A continental-scale hydrology
547 and water quality model for Europe: Calibration and uncertainty of a high-resolution large-scale SWAT model. *Journal of*
548 *Hydrology* 524, 733-752.

549 Arabi, M., Govindaraju, R.S., Hantush, M.M., and B.A. Engel (2006), Role of watershed subdivision on modeling the
550 effectiveness of best management practices with SWAT. *Journal of the American Water Resources Association* 42(2), 513-
551 528.

552 Bailey, R.T., Wible, T.C., Arabi, M., Records, R.M., and J. Ditty (2016), Assessing regional-scale spatio-temporal patterns of
553 groundwater-surface water interactions using a coupled SWAT-MODFLOW model. *Hydrological Processes* 30, 4420-4433.

554 Brown, S.C., Versace, V.L., Lester, R.E. and Walter, M.T. (2015), Assessing the impact of drought and forestry on streamflows
555 in south-eastern Australia using a physically based hydrological model, *Environmental Earth Sciences*, 74(7), 6047-6063,
556 available: <http://dx.doi.org/10.1007/s12665-015-4628-8>.

557 Burkhalter, J. P., and Gates, T. K. (2006), Evaluating regional solutions to salinization and waterlogging in an irrigated river
558 valley. *Journal of Irrigation and Drainage Engineering*, 132(1): 21 – 30.

559 Dechmi, F., and A. Skhiri (2013), Evaluation of best management practices under intensive irrigation using SWAT model.
560 *Agricultural Water Management* 123, 55-64.

561 Ficklin, D.L., Luo, Y., Luedeling, E. and Zhang, M. (2009), Climate change sensitivity assessment of a highly agricultural
562 watershed using SWAT, *Journal of Hydrology*, 374(1-2), 16-29, available: <http://dx.doi.org/10.1016/j.jhydrol.2009.05.016>.

563 Frasier, W.M., Waskom, R.M., Hoag, D.L., and T.A. Bauder (1999), *Irrigation Management in Colorado: Survey Data and*
564 *Findings*. Technical Report TR99-5 Agricultural Experiment Station, Colorado State University. Fort Collins, CO.

565 Gates, T.K., Burkhalter, J.P., Labadie, J.W., Valliant, J.C., Broner, I. (2002), Monitoring and modeling flow and salt transport in
566 a salinity-threatened irrigated valley, *Journal of Irrigation and Drainage Engineering*, Vol. 128, No. 2, 88-99.

567 Gates, T.K., Steed, G.H., Niemann, J.D., Labadie, J.W. (2016), *Data for Improved Water Management in Colorado's Arkansas*
568 *River Basin*, Hydrological and Water Quality Studies, Colorado State University.

569 Goff, K., M.E. Lewis, M.A. Person, and L.F. Konikow (1998), Simulated effects of irrigation on salinity in the Arkansas River
570 Valley in Colorado. *Ground Water* 36:76-86.

571 Haddeland, I., Heinke, J., Voss, F., Eisner, S., Chen, C., Hagemann, S. and Ludwig, F. (2012), Effects of climate model
572 radiation, humidity and wind estimates on hydrological simulations, *Hydrology and Earth System Sciences*, 16(2), 305-318,
573 available: <http://dx.doi.org/10.5194/hess-16-305-2012>.

574 Jyrkama, M.I. and Sykes, J.F. (2007), The impact of climate change on spatially varying groundwater recharge in the grand river
575 watershed (Ontario), *Journal of Hydrology*, 338(3-4), 237-250, available: <http://dx.doi.org/10.1016/j.jhydrol.2007.02.036>.

576 Kaledhonkar, M. J., and Keshari, A. K. (2006), Regional salinity modeling for conjunctive water use planning in Kheri
577 command. *J. Irrig. Drain. Eng.*, 132(4), 389–398.

578 Kaledhonkar, M.J., Sharma, D.R., Tyagi, N.K., Kumar, A., and Van Der Zee S.E.A.T.M. (2012), Modeling for conjunctive use
579 irrigation planning in sodic groundwater areas. *Agricultural Water Management* 107, 14-22.

580 Konikow, L.F., and M. Person (1985), Assessment of long-term salinity changes in an irrigated stream aquifer system. *Water*
581 *Resources Research* 21:1611-1624.

582 Maringanti, C., Chaubey, I., and J. Popp (2009), Development of a multiobjective optimization tool for the selection and
583 placement of best management practices for nonpoint source pollution control. *Water Resources Research*,
584 [doi.org/10.1029/2008WR007094](http://dx.doi.org/10.1029/2008WR007094).

585 Martin CA, Gates TK (2014), Uncertainty of canal seepage losses estimated using flowing water balance with acoustic Doppler
586 devices. *Journal of hydrology* 517: 746-761.

587 Morway, E.D., Gates, T.K. (2012), Regional assessment of soil water salinity across an intensively irrigated river valley, *Journal*
588 *of Irrigation and Drainage Engineering*, Vol. 138, No. 5, 393-405.

589 Morway, E.D., Gates, T.K. and Niswonger, R.G. (2013), Appraising options to reduce shallow groundwater tables and enhance
590 flow conditions over regional scales in an irrigated alluvial aquifer system. *Journal of hydrology*, 495, 216-237.

591 Mueller Price, J., & Gates, T.K., 2007, Assessing uncertainty in mass balance calculation of river nonpoint source loads. *Journal*
592 *of Environmental Engineering*, 134(4), 247-258.

593 Napoli, M., Massetti, L, and S. Orlandini (2017), Hydrological response to land use and climate changes in a rural hilly basin in
594 Italy. CATENA 157, 1-11.

595 Neitsch, S.L., J.G. Arnold, J.R. Kiniry, J.R. Williams (2011), Soil and Water Assessment Tool Theoretical Documentation,
596 Version 2009. Temple, Tex.: Texas Water Resources Institute Technical Report No. 406.

597 National Land and Water Resources Audit, 2001, Australian Government.

598 Oosterbaan, R. J., 2005, SAHYSMOD (version 1.7a), Description of principles, user manual and case studies, International
599 Institute for Land Reclamation and Improvement, Wageningen, Netherlands, 140.

600 Parkhurst, D.L., Appelo, C.A.J. (2013), Description of Input and Examples for PHREEQC Version 3- A Computer Program for
601 Speciation, Batch-Reaction, One-Dimensional Transport, and Inverse Geochemical Calculations, Chapter 43 of Section A,
602 Groundwater, Book 6, Modeling Techniques.

603 Paz-García J., Johannesson, B., Ottosen, L., Ribeiro, A., Rodríguez-Maroto, J. (2013), Computing multi-species chemical
604 equilibrium with an algorithm based on the reaction extents, Computers & Chemical Engineering, Vol: 58 pp: 135-143.

605 Rasouli, F., Pouya, A.K., and J. Šimůnek (2013), Modeling the effects of saline water use in wheat-cultivated lands using the
606 UNSATCHEM model. Irrigation Science 31(5), 1009-1024.

607 Schoups, G., Hopmans, J.W., Young, C.A., Vrugt, J.A., Wallender, W.W., Tanji, K.K., and S. Panday (2005), Sustainability of
608 irrigated agriculture in the San Joaquin Valley, California. Proceedings of the National Academy of Sciences of the United
609 States of America, 102(43), 15352-15356.

610 Schoups, G., Hopmans, J.W. and Tanji, K.K. (2006), Evaluation of model complexity and space–time resolution on the
611 prediction of long-term soil salinity dynamics, western San Joaquin Valley, California. Hydrological Processes, 20(13),
612 2647-2668.

613 Šimůnek, J., and D. L. Suarez (1994), Two-dimensional transport model for variably saturated porous media with major ion
614 chemistry, Water Resources Research, 30(4), 1115-1133.

615 Šimůnek, J., M. Šejna, and M. Th. van Genuchten (2012), The UNSATCHEM Module for HYDRUS (2D/3D) Simulating Two-
616 Dimensional Movement of and Reactions Between Major Ions in Soils, Version 1.0, PC Progress, Prague, Czech Republic,
617 54 pp.

618 Singh, A., Panda, S.N. (2012), Integrated salt and water balance modeling for the management of waterlogging and salinization;
619 I: Validation of SAHYSMOD, Journal of Irrigation and Drainage Engineering, Vol. 138, 955-963.

620 Susfalk R, Sada D, Martin C, Young MH, Gates T, Rosamond C, Mihevc T, Arrowood T, Shanafield M, Epstein B, Fitzgerald B.
621 (2008), Evaluation of linear anionic polyacrylamide (LA-PAM) application to water delivery canals for seepage reduction.
622 Desert Research Institute. DHS Publication No. 41245.

623 Tavakoli-Kivi, S. (2018), ~~Simulating the fate of~~ Bailey, R.T., and T.K. Gates (2019). A salinity reactive transport of salinity
624 ~~species in a semi-arid and equilibrium chemistry model for regional-scale agricultural groundwater system: model~~
625 ~~development and application. PhD Dissertation, Dept. of Civil and Environmental Engineering, Colorado State University,~~
626 ~~Fort Collins, CO systems. Journal of Hydrology 572, 274-293.~~

627 Tanji and Kielen (2002), Agricultural drainage water management in arid and semi-arid areas, FAO Irrigation and Drainage
628 Paper 61, Rome, 2002.

629 Tweed, S., Leblanc, M. and Cartwright, I. (2009), Groundwater-surface water interaction and the impact of a multi-year drought
630 on lakes conditions in South-East Australia, Journal of Hydrology, 379(1-2), 41-53, available:
631 <http://dx.doi.org/10.1016/j.jhydrol.2009.09.043>.

632 Ullrich, A. and M. Volk (2009), Application of the Soil and Water Assessment Tool (SWAT) to predict the impact of alternative
633 management practices on water quality and quantity. *Agricultural Water Management* 96(8), 1207-1217.

634 Umali, D.L. (1993), Irrigation- induced salinity: A growing problem for development and the environment: Technical Paper
635 215. World Bank, Washington, DC.

636 Wagenet, R.J., and J.L. Hutson (1987), LEACHM-Leaching estimation and chemistry model. Center Environ. Res., Cornell
637 Univ., Ithaca, NY.

638 Wei, X., Bailey, R.T. and A. Tasdighi (2018), Using the SWAT model in intensively managed irrigated watersheds: model
639 modification and application. *Journal of Hydrologic Engineering* 23(10): 04018044.

640 Zhao, A., Zhu, X., Liu, X., Pan, Y., and D. Zuo (2016), Impacts of land use change and climate variability on green and blue
641 water resources in the Weihe River Basin of northwest China. *CATENA* 137, 318-327.

642 Zuo, D., Xu, Z., Yao, W., Jin, S., Xiao, P., and D. Ran (2016), Assessing the effects of changes in land use and climate on runoff
643 and sediment yields from a watershed in the Loess Plateau of China. *Science of the Total Environment* 544, 238-250.

644

645

646

647

648

649

650

651

652

653

654

655

656

657

658

659

660

661

662

663

664

665

666

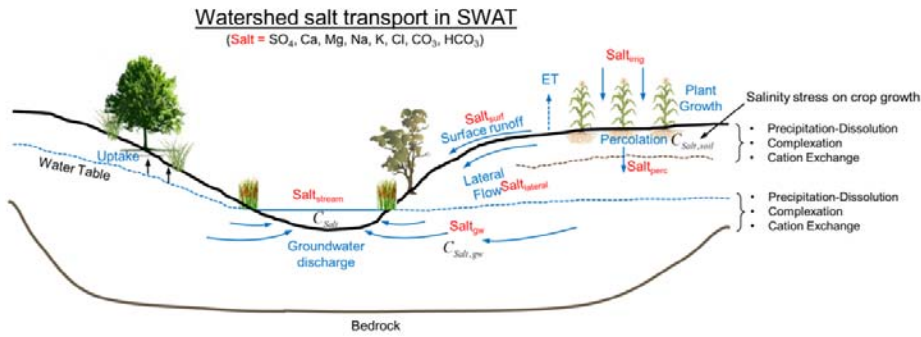
667

668

669

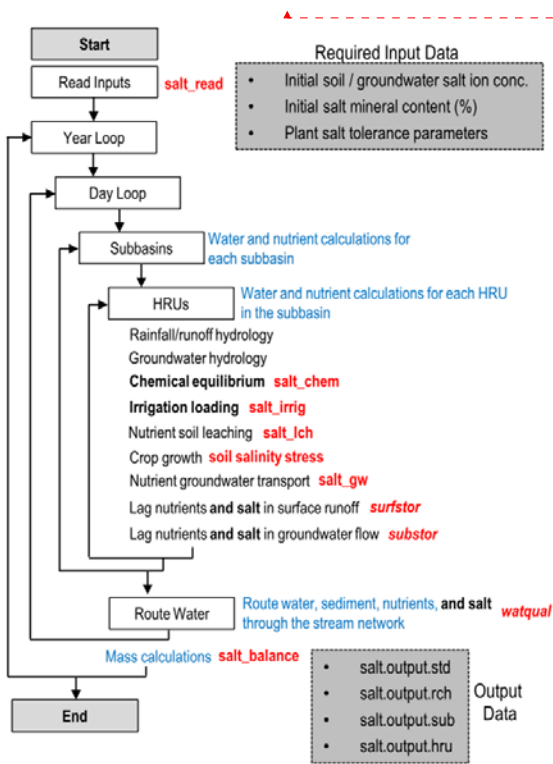
670

671



672
673
674
675
676
677

Figure 1. Schematic showing a cross-section of an irrigated stream-aquifer system and the major transport pathways of salt, which consists of the eight major ions of SO₄, Ca, Mg, Na, K, Cl, CO₃, HCO₃. The concentration of each ion is also governed by equilibrium chemistry reactions such as precipitation-dissolution, complexation, and cation exchange within the soil profile and within the aquifer.

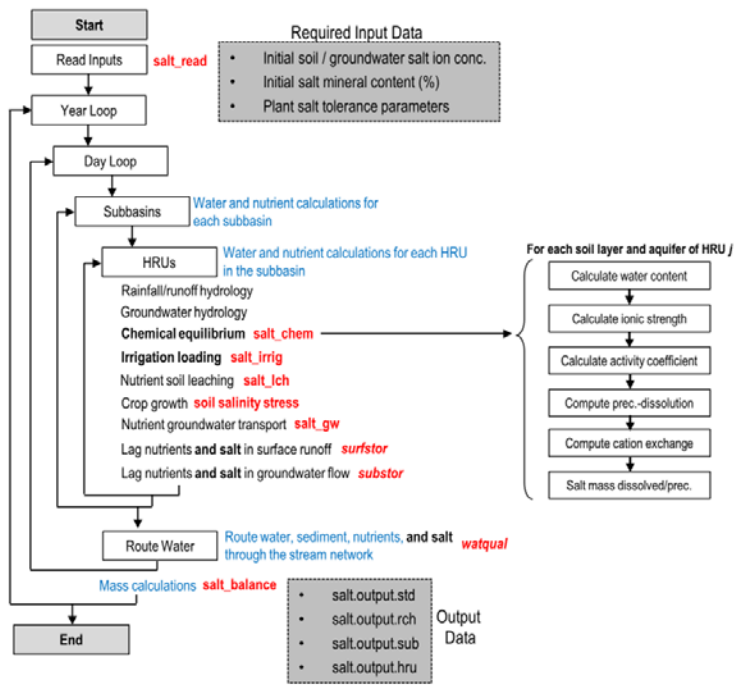


Formatted: Font: Not Bold

Formatted: Centered, Indent: Left: 0", First line: 0", Don't add space between paragraphs of the same style, Line spacing: single

678
679
680
681

682
683



684
685
686
687
688
689

Figure 2. Data flow within the SWAT-Salt modeling code. Boxes and text in black and blue indicate original SWAT loops and subroutines. Text in red indicates either new or modified subroutines for the Salinity module. The required input data for the salinity module is shown in the upper shaded box, whereas the generated output files are shown in the lower shaded box.

Formatted: Left, Indent: Left: 0", First line: 0", Don't add space between paragraphs of the same style, Line spacing: single

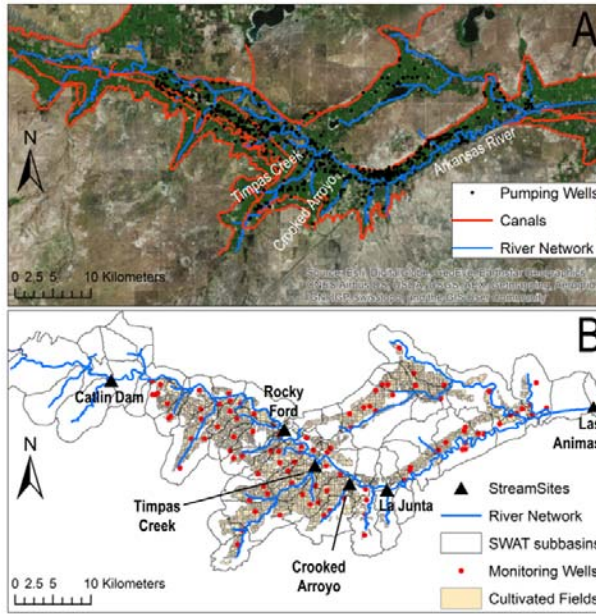
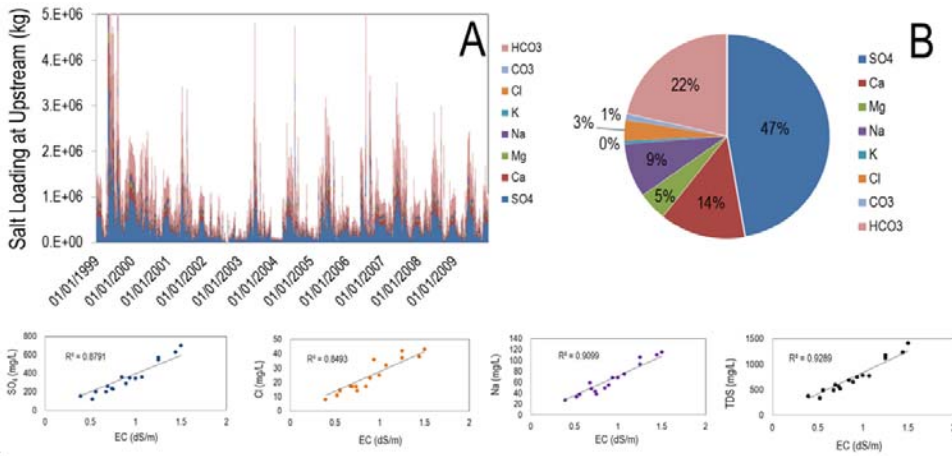


Figure 3. Map of study region within the Lower Arkansas River Valley of Colorado, showing (A) Arkansas River and tributaries, irrigation canals, and pumping wells, and (B) cultivated fields, monitoring wells where groundwater is sampled for salt ions, sampling sites where surface water is sampled for salt ions, and SWAT subbasins.

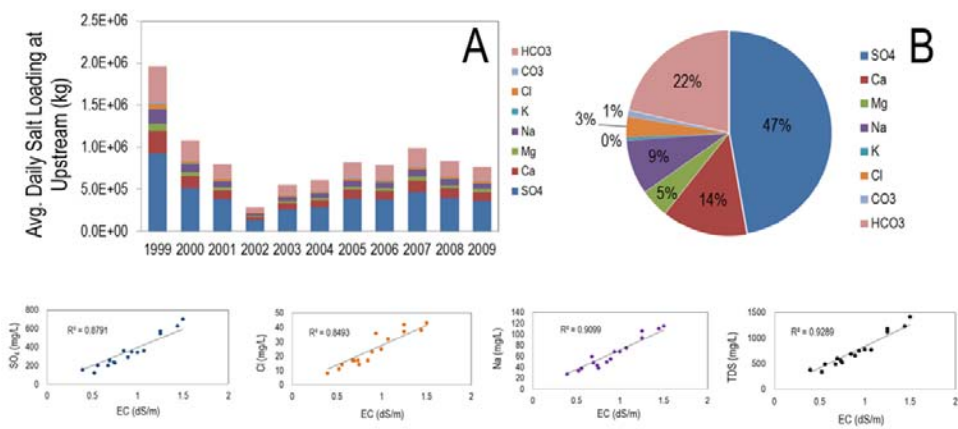
Formatted: Centered, Indent: Left: 0", First line: 0", Don't add space between paragraphs of the same style, Line spacing: single



690
691
692
693
694
695
696
697

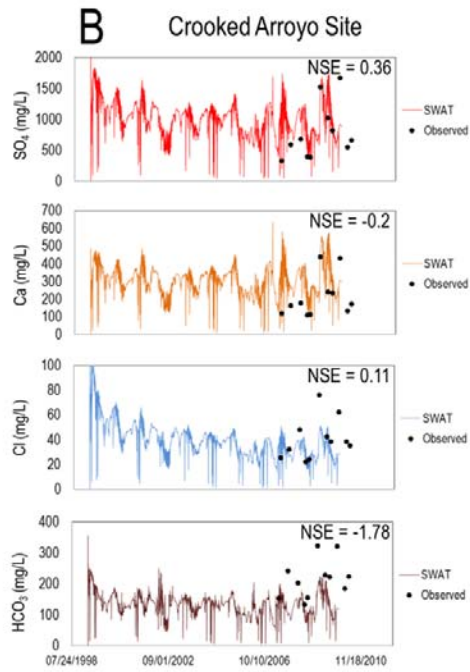
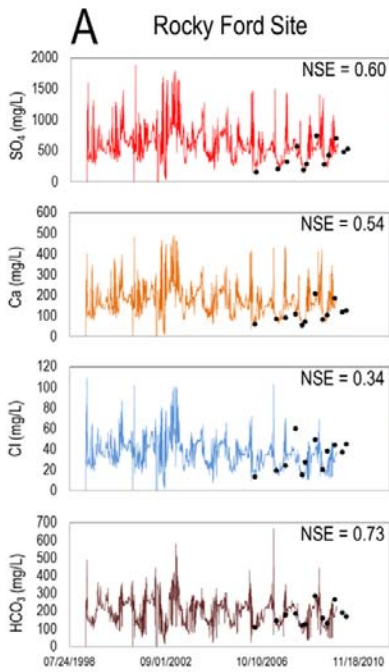
698
699
700
701
702
703
704

705
706
707
708
709
710
711
712
713
714
715
716
717

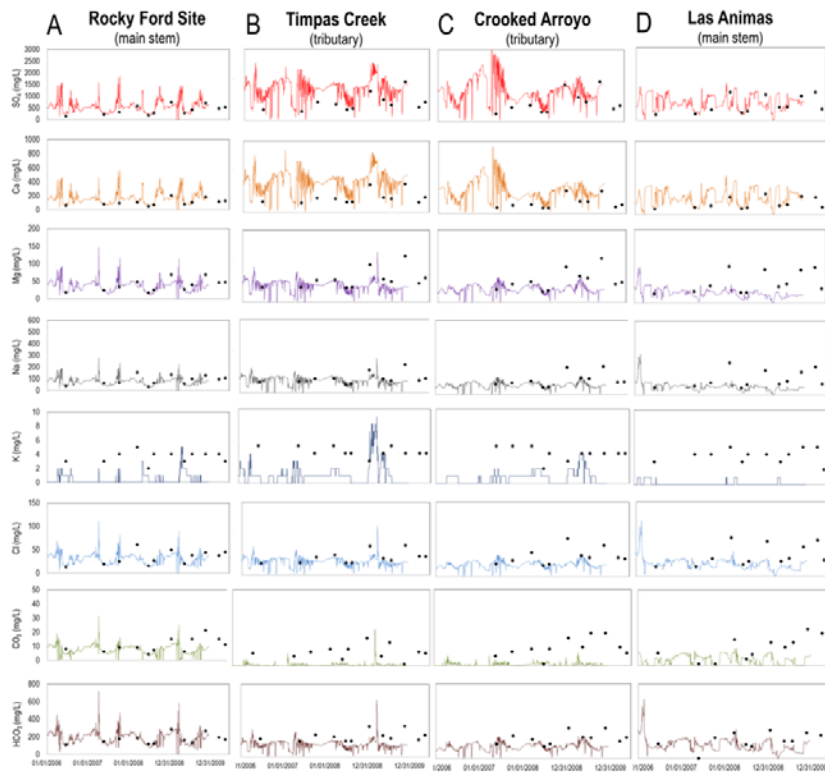


718
719
720
721
722
723
724

Figure 4. Data summarizing the specified loading of salt (kg/day) at the Catlin Dam gage site, using observed EC (dS/m) and stream discharge (m³/day) data: (A) daily loading of salt ion, (B) percentage of total salt loading attributed to each salt ion, (bottom charts) example regression plots used to relate EC to salt ion concentration.

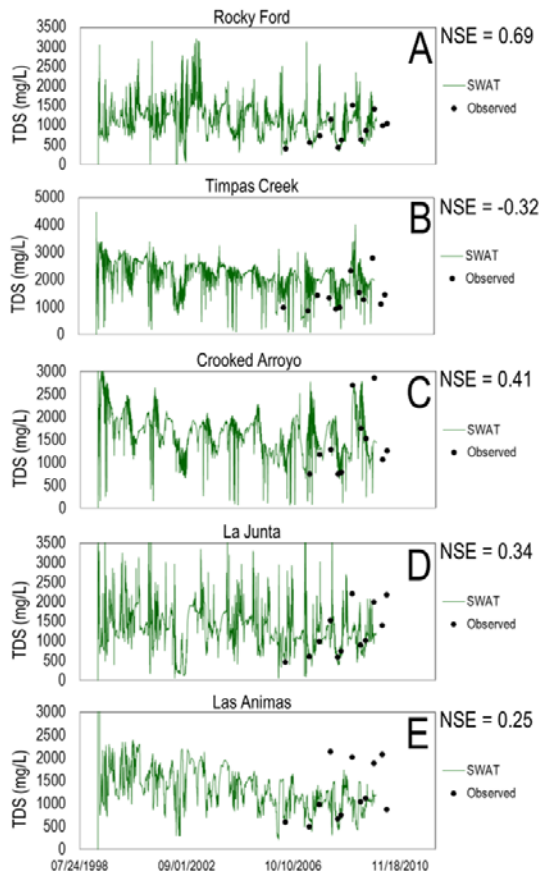


725
726
727
728
729
730
731
732
733
734
735
736
737
738
739
740
741
742
743
744
745
746
747
748
749
750
751



752
 753 **Figure 5.** Time series of simulated and observed concentration (mg/L) for each of selected the 8 major salt ions for the (A) Rocky
 754 Ford sampling site along the Arkansas River (see Fig. 3) and the (B) Timpas Creek site, (C) Crooked Arroyo sampling site. The
 755 Nash Sutcliffe model efficiency coefficient (NSE) is shown for each plot site, and (D) Las Animas site. Simulated hydrographs
 756 for these sites are in Wei et al. (2018).
 757

Formatted: Centered



758
 759
 760
 761
 762
 763
 764
 765
 766
 767
 768
 769

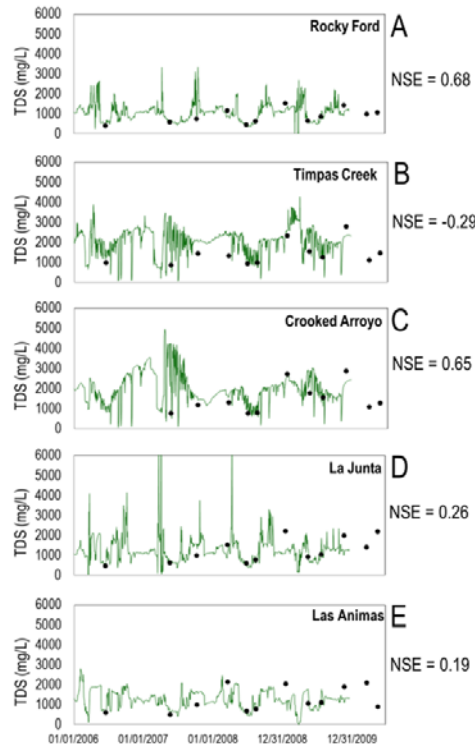


Figure 6. Simulated and observed total dissolved solids (TDS) (mg/L) in the five stream sampling sites along the Arkansas River (A, D, E), and two tributaries (B, C). See Fig. 3 for locations. TDS is the summation of the concentration of the 8 salt ions. The Nash-Sutcliffe model efficiency coefficient (NSE) is shown for each plot.

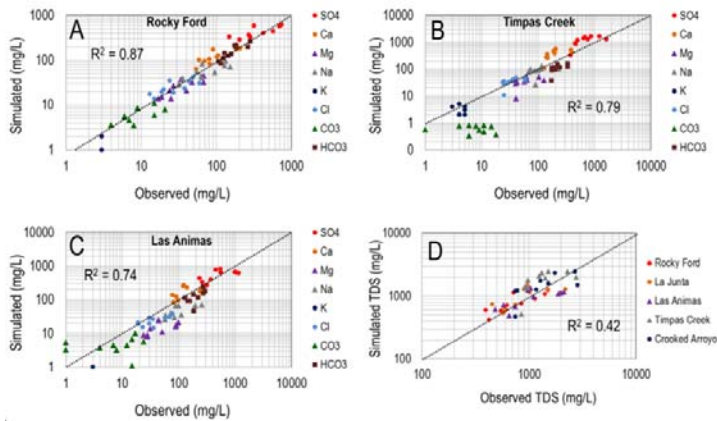
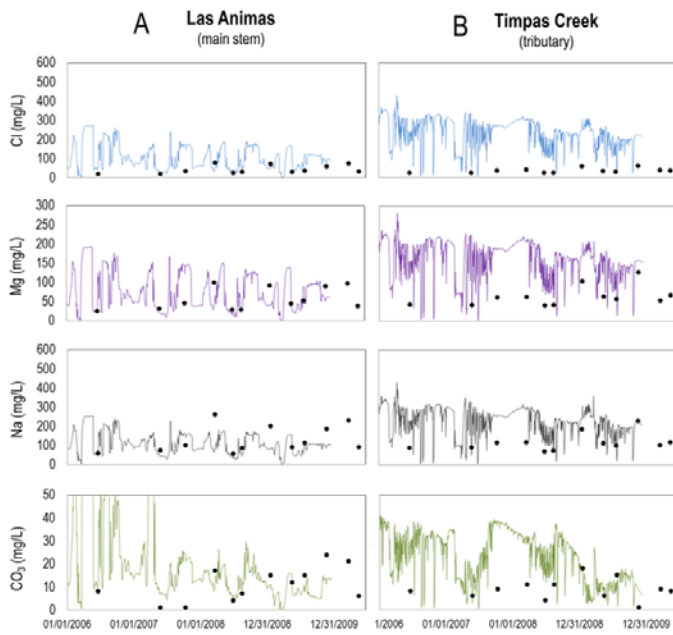


Figure 7.

Formatted: Centered
 Formatted: Add space between paragraphs of the same style

779
780
781
782
783
784
785
786
787
788
789
790
791



792
793
794
795
796
797
798
799
800
801

Figure 7. Time series of simulated and observed concentration (mg/L) for each of the 8 major salt ions for the (A) Las Animas site and (B) Timpas Creek site, for the model scenario of using 0.0002 soil bulk fractions for $MgCO_3$, $MgSO_4$, and NaCl. For the baseline model, these fractions were set to 0.00.

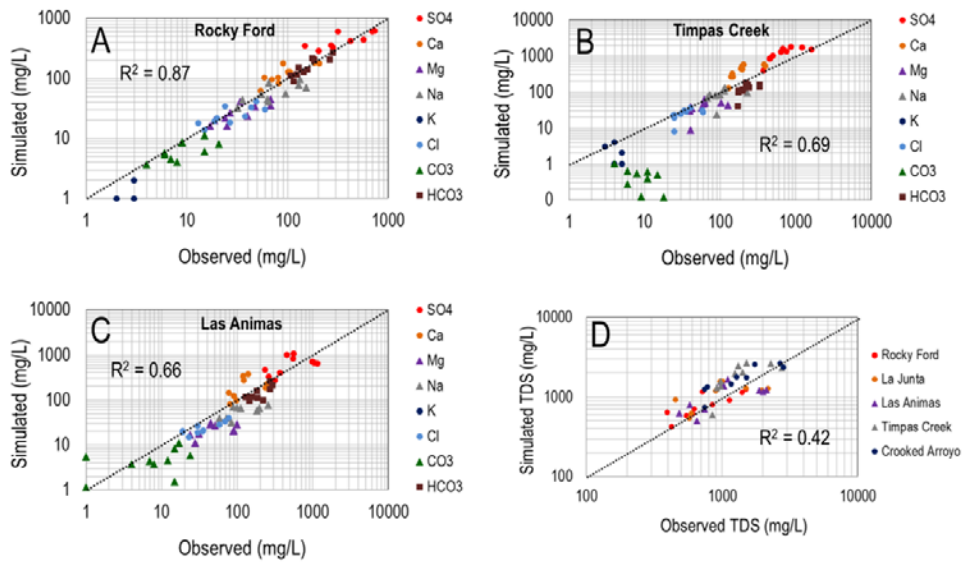
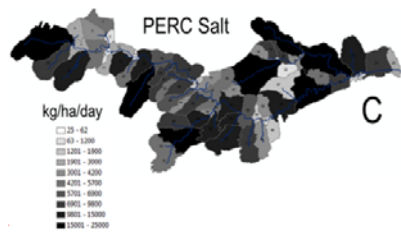
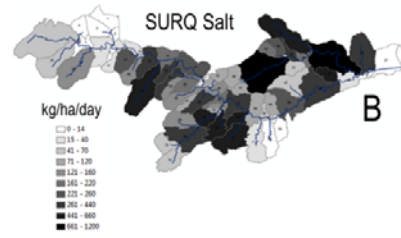
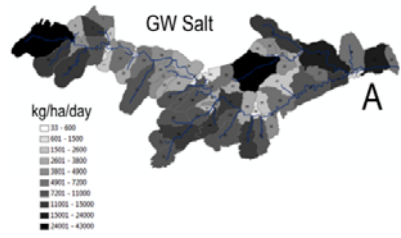


Figure 8. Log-log plots of observed vs. simulated salt ion concentration for the (A) Rocky Ford, (B) Timpas Creek, and (C) Las Animas surface water sampling sites. (D) shows the comparison of TDS for the five sites.

802
803
804
805
806
807
808



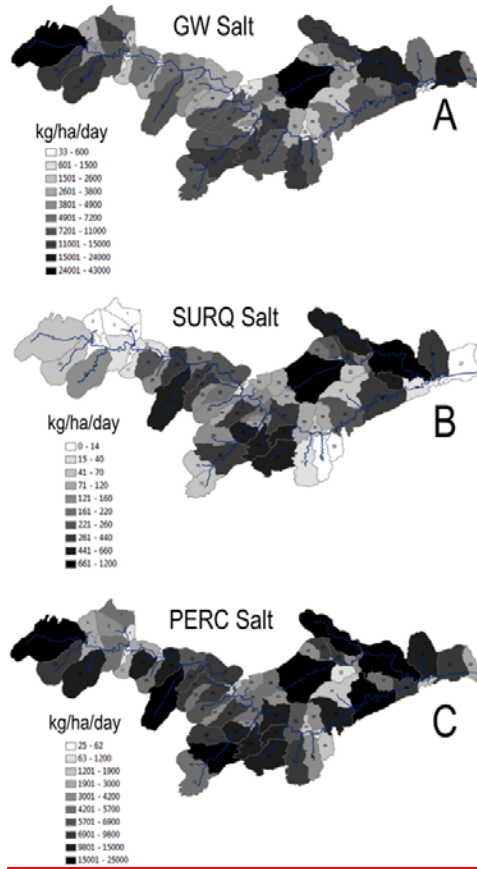
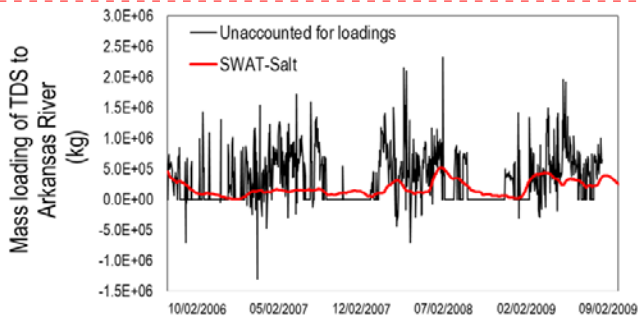


Figure 89. Average daily loading (kg/ha) of salt by subbasin to (A) stream network via groundwater discharge, (B) stream network via surface runoff, (C) groundwater via soil percolation.

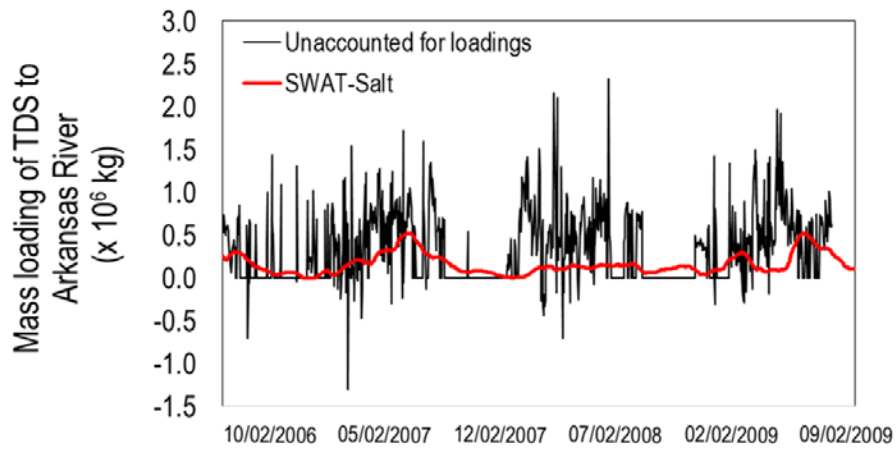


Formatted: Font color: Red
 Formatted: Left, Indent: Left: 0", First line: 0", Line spacing: single

810
811
812
813

814
815
816
817
818

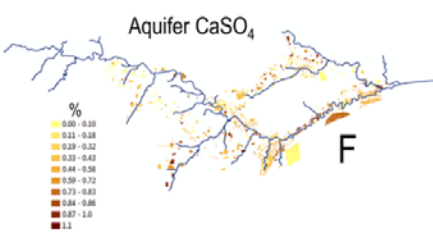
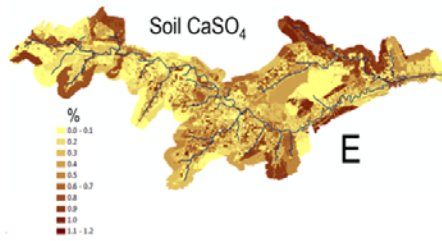
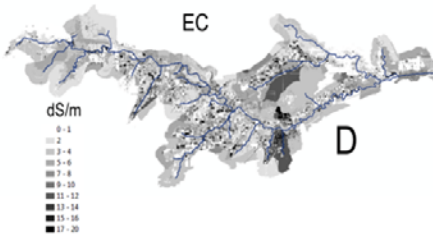
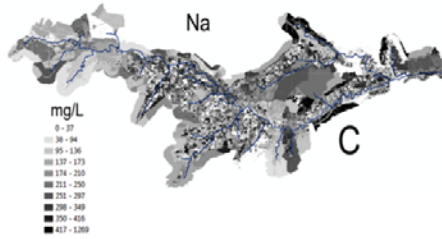
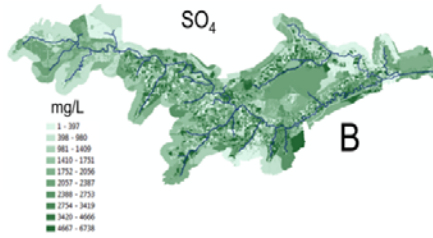
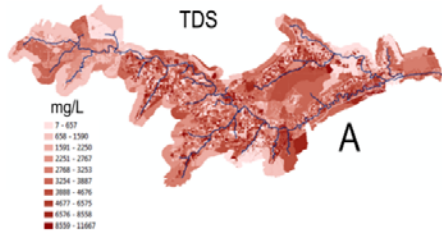
819
820
821
822
823
824
825
826
827
828



829
830
831
832
833
834
835
836
837

Figure 9.10. Simulated daily mass loading of TDS (kg) to the Arkansas River via groundwater discharge for the SWAT model with uniform initial salt concentrations. Results from a salt mass balance calculation on the Arkansas River also are plotted, showing the unaccounted for TDS loadings (groundwater, surface runoff, small inflows) in the Arkansas River.

Formatted: Font color: Red
Formatted: Add space between paragraphs of the same style



838
839
840
841
842
843
844
845
846
847

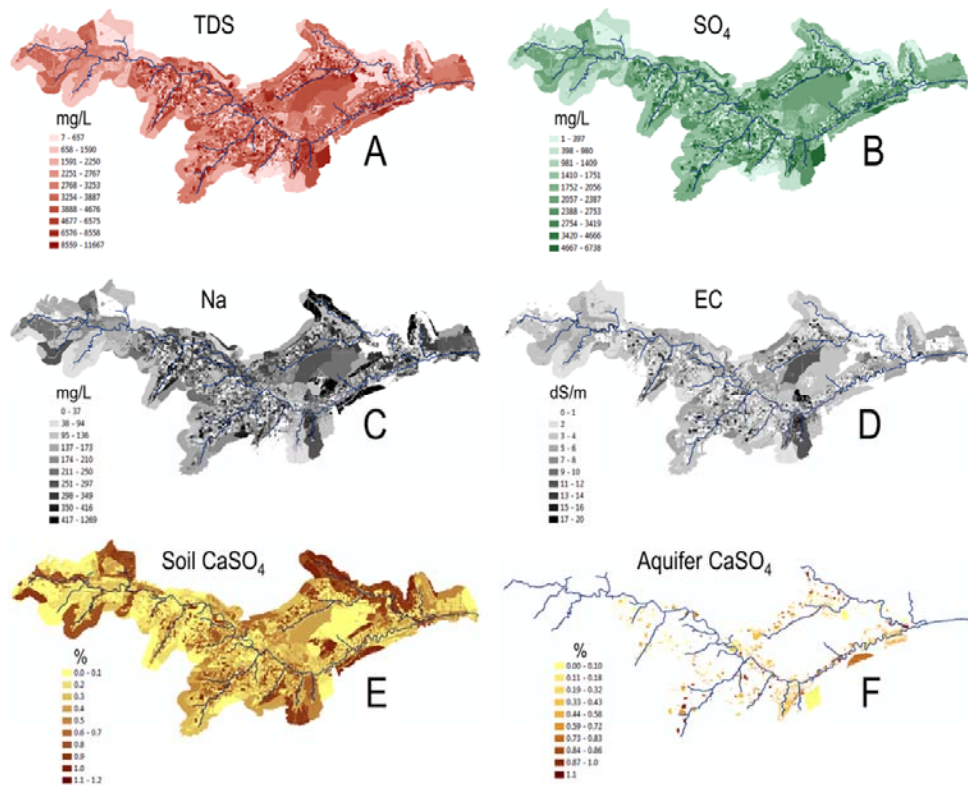
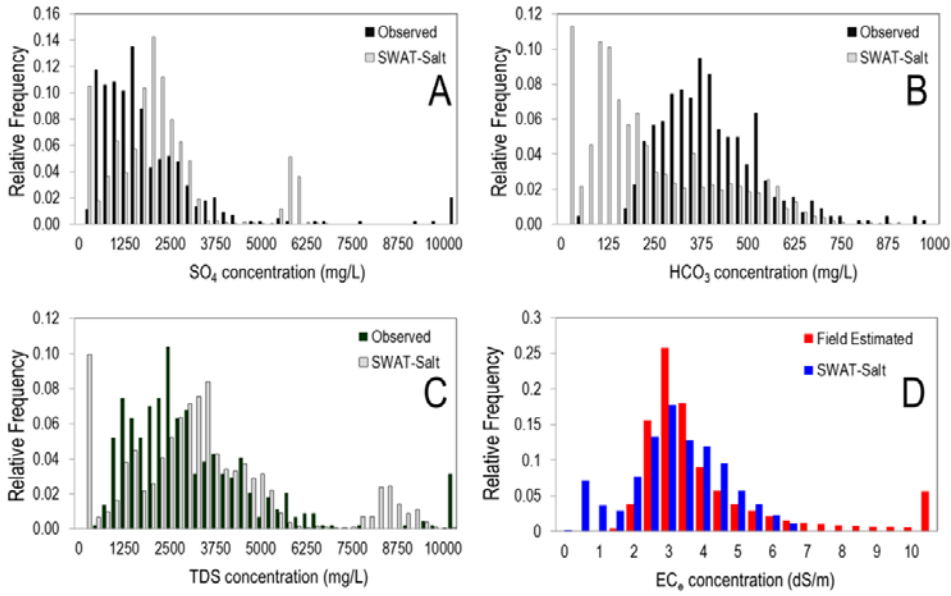
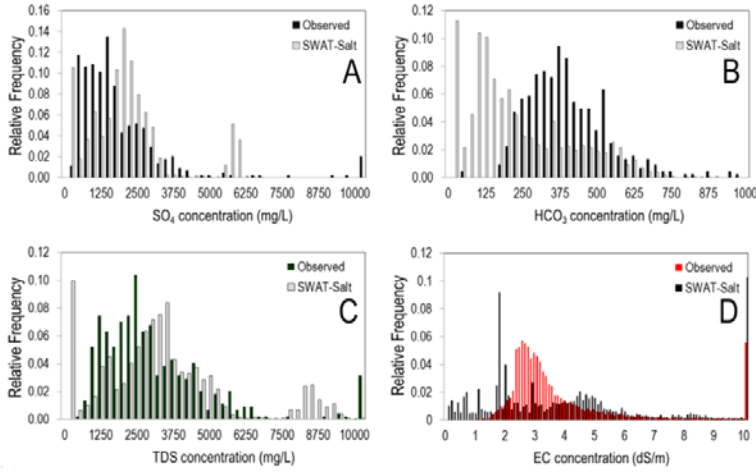


Figure 1911. HRU average concentration over the 2006-2009 simulation period for (A) groundwater TDS (mg/L), (B) groundwater SO₄ (mg/L), (C) groundwater Na (mg/L), and (D) soil water electrical conductivity EC (dS/m). (E) and (F) show percentage of soil bulk volume and aquifer bulk volume, respectively, that is CaSO₄, near the end of the simulation in May 2010.

Formatted: Left, Indent: Left: 0", First line: 0", Don't add space between paragraphs of the same style, Line spacing: single

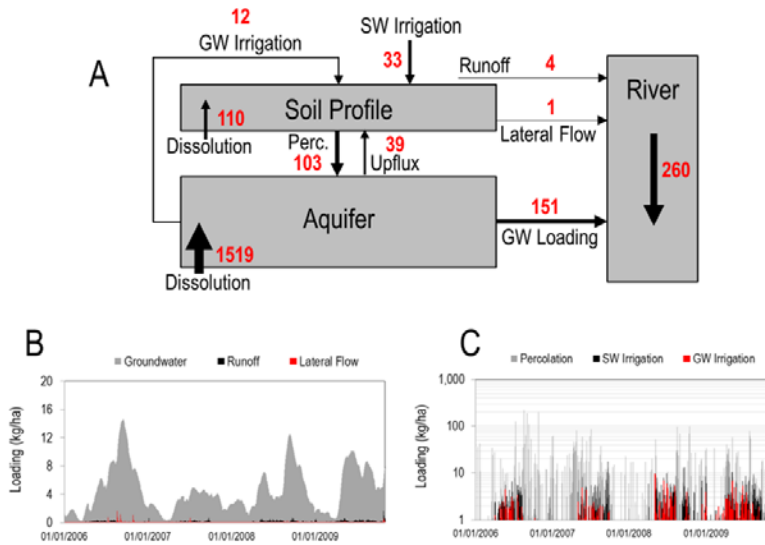
848
849
850
851
852
853
854
855

856
857
858
859
860
861
862
863
864
865
866
867
868



869
870

871 **Figure 1412.** Relative frequency plots of simulated and observed values of (A) SO_4 groundwater concentration, (B) HCO_3
 872 groundwater concentration, (C) TDS groundwater concentration, and (D) EC_{e} soil water concentration—Simulated of a
 873 saturated paste. Groundwater simulated values are taken from each HRU of the SWAT simulation, on days for which observed
 874 values are available. For soil EC_{e} values are taken only from HRUs that coincide with cultivated fields.
 875
 876
 877
 878



879
 880
 881
 882
 883
 884
 885
 886
 887
 888
 889
 890
 891
 892
 893
 894
 895

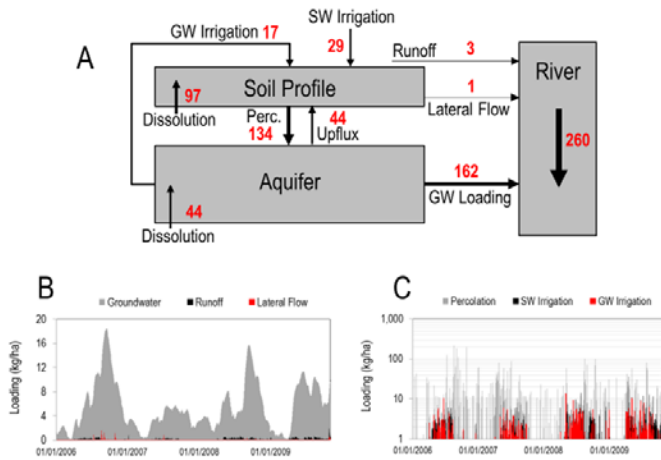
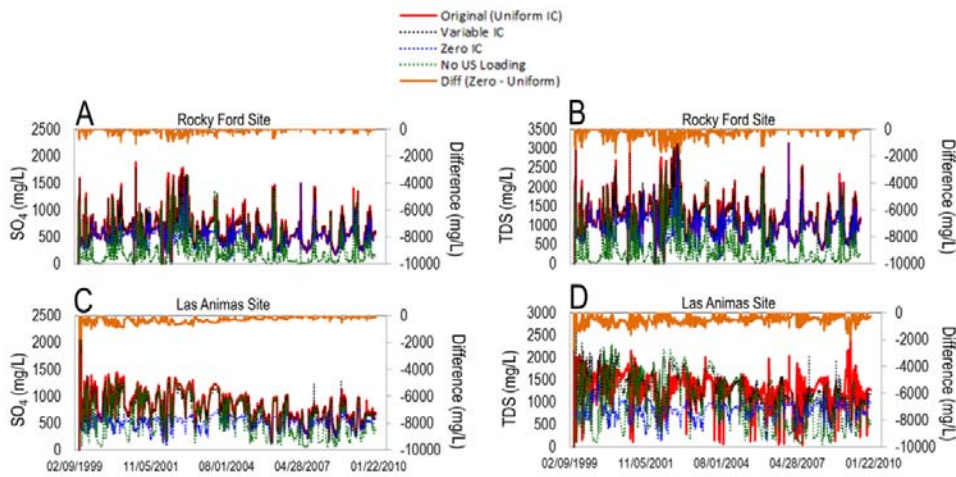
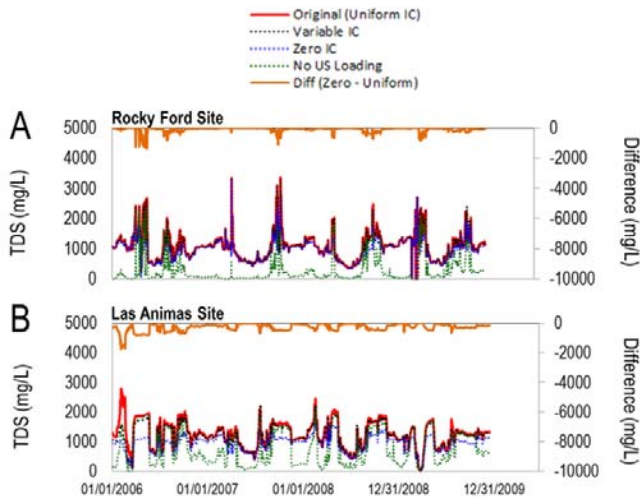
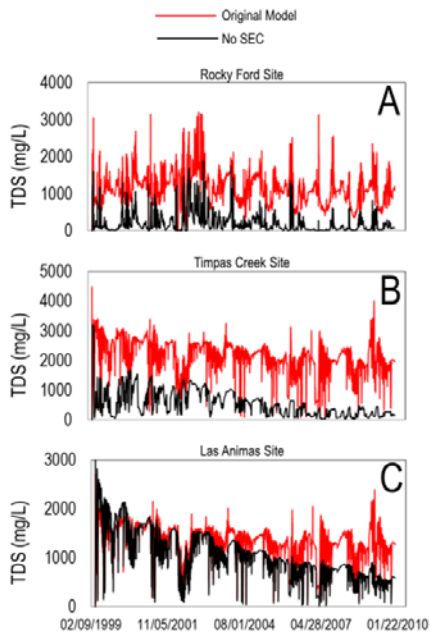


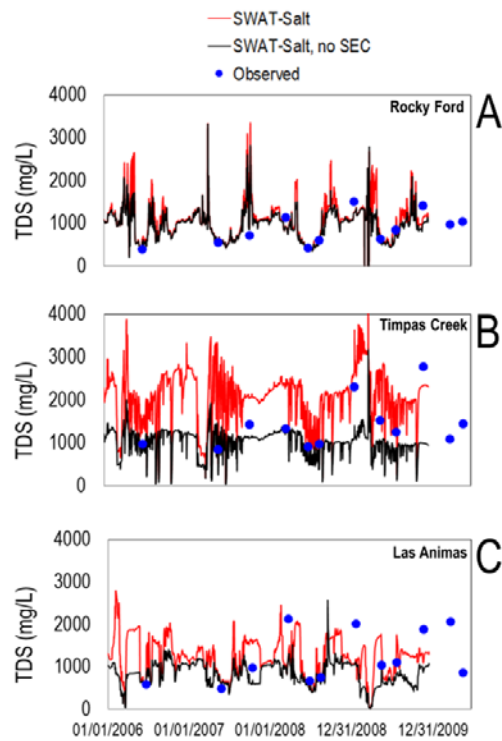
Figure 1213. Magnitude of salt balance components in the watershed model for TDS, showing (A) relative salt flux between soil storage compartments in the watershed for each salt transport pathway; (B) daily loading (kg/ha) of salt in groundwater, surface runoff, and lateral flow to streams; and (C) daily loading (kg/ha) of salt in percolation water (from bottom of soil profile to the aquifer), irrigation derived from irrigation canals, and irrigated derived from groundwater pumping.





910
911
912 **Figure 1314.** Simulated in-stream SO_4 and TDS concentration (mg/L) at the Rocky Ford Site and the Las Animas Site gage sites
913 along the Arkansas River for four scenarios: uniform initial conditions (IC) of salt soil water and groundwater concentrations,
914 corresponding to the original simulation; variable IC; IC = 0; and no upstream loading of salt at the Catlin Dam site. Also show
915 is the difference between the IC = 0 scenario and the original scenario.
916
917
918





920
 921 **Figure 1415.** Simulated in-stream TDS concentration (mg/L) at the (A) Rocky Ford Site, (B) Timpas Creek Site, and (C) Las
 922 Animas Site for the original simulation (red line) and a simulation without including equilibrium chemistry (SEC module) (black
 923 line). The measured TDS values also are shown.
 924

925
926
927
928
929
930
931
932
933
934
935
936
937
938
939
940
941
942
943
944
945
946
947
948
949
950
951
952
953
954
955
956

Table 1. Groups and Species included in the Salinity Equilibrium Chemistry (SEC) module for SWAT.

| Group | Species |
|-------------------|--|
| Aqueous Species | Ca^{2+} , Mg^{2+} , Na^+ , K^+ , SO_4^{2-} , CO_3^{2-} , HCO_3^- , Cl^- |
| Solid Species | CaSO_4 , CaCO_3 , MgCO_3 , NaCl , MgSO_4 |
| Complexed Species | CaSO_4^0 , MgSO_4^0 , CaCO_3^0 , CaHCO_3^+ , MgCO_3^0 , MgHCO_3^+ , NaSO_4^- , KSO_4^- , NaHCO_3^0 , NaCO_3^0 |
| Exchanged Species | Ca, Mg, Na, K |

Formatted: Font: Bold
Formatted: Table, Add space between paragraphs of the same style

957
 958
 959
 960
 961
 962
 963
 964
 965
 966
 967
 968
 969
 970
 971
 972
 973
 974
 975
 976
 977
 978
 979
 980
 981
 982
 983
 984
 985
 986
 987
 988

Table 2. Summary statistics for observed (monitoring well) and simulated (SWAT) salinity concentrations in groundwater.

| Species | Maximum (mg/L) | | Average (mg/L) | |
|------------------|----------------|-----------|----------------|-----------|
| | Observed | Simulated | Observed | Simulated |
| Na | 2606 | 1269677 | 402 | 187247 |
| Ca | 767 | 2234233 | 353 | 653628 |
| Mg | 1019 | 497341 | 191 | 78117 |
| K | 85 | 277353 | 4 | 96 |
| SO ₄ | 6510 | 67386132 | 1878 | 20582149 |
| CO ₃ | 42 | 84 | 2 | 0 |
| HCO ₃ | 2362 | 18281232 | 410 | 225299 |
| Cl | 1803 | 480225 | 95 | 6563 |
| TDS | 13007 | 116679920 | 3334 | 32763508 |

Formatted: Not Superscript/ Subscript
 Formatted: Not Superscript/ Subscript
 Formatted: Not Superscript/ Subscript

989 **RC1:**

990 General comments: This work focused on developing a new watershed-scale salt ion fate and transport
991 model based on SWAT model, which can account for salt loading for each major hydrologic pathway in a
992 watershed setting for each major salt ion (SO₄, Ca, Mg, Na, K, Cl, CO₃, HCO₃). This is very interesting
993 work trying to quantitatively estimate the chemical and physical characteristics of the common ions, which
994 is important for soil salinity control in semi-arid areas with shallow water table depth. Since most current
995 research mainly focused on the transport of total salt in surface and subsurface system while not distinguish
996 the contribution of different ions and the reactions, this work provides the new view and method for soil
997 salinity control. I would think this work is valuable and can be published by major revision.

998 [We thank the reviewer for the comments.](#)

999
1000 Major revisions:

1001
1002 (1) The numerical integrating method to couple the ion reactions and water flow and solute transport model
1003 SWAT should be illustrated in details. This will help for understanding the model.

1004 [Response:](#) The `salt_chem` subroutine includes all salt chemistry reactions. The details of this subroutine
1005 have been added to Figure 2, and the following text was added to Section 2.2.7:

1006
1007 **Lines 223-229:**

1008 *“The salinity chemistry reactions (precipitation-dissolution, complexation, cation exchange) are simulated*
1009 *for each HRU within the salt_chem subroutine (see Figure 2). Within this subroutine, the chemistry*
1010 *reactions are applied to the current simulated concentration values of the 5 salt minerals and the 8 salt*
1011 *ions for each soil layer and aquifer, to calculate new concentration values. These new concentration values*
1012 *are then used to simulate salt leaching (salt_lch subroutine) and salt ion loading in surface runoff*
1013 *(surfstor) and groundwater flow (salt_gw, substor) (Figure 2). At the end of each daily time step, the*
1014 *simulated salt ion mass (kg) in each transport pathway (irrigation, leaching, runoff, percolation, lateral*
1015 *flow, groundwater flow, dissolution/precipitation) is stored for mass balance assessment and output.”*

1016
1017 (2) How many parameters were included in this model? There is no any introduction about the parameters
1018 used in the model calibration and validation, e.g., the salinity percolation coefficient β_{Si} , the surface runoff
1019 lag coefficient $surlag$. How do you set the value of these parameter, which are important to judge the
1020 reasonability of the model?

1021 [Response:](#) The calibration and testing of the original SWAT model was presented in Wei et al. (2018). In
1022 summary, calibration was performed using SWAT-CUP. Calibration was performed for 2001-2003 using
1023 the simulated and observed streamflow at 3 stream gages in the model domain. Twenty parameters were
1024 adjusted to minimize the objective function (see Table 4 in Wei et al., 2008). The high-sensitive parameters
1025 include SCS runoff curve number, Manning’s n value for the main channel, effective hydraulic
1026 conductivity of the channel, initial volume of groundwater, recharge delay time, fraction of deep aquifer
1027 percolation, and snowfall temperature. The following text has been added to the revised manuscript:

1028
1029 **Lines 291-298:**

1030 *“Calibration was performed using SWAT-CUP (Abbaspour et al., 2008) using the observed streamflow at*
1031 *the Rocky Ford, Las Animas, and Timpas Creek stations. Twenty parameters were targeted for*
1032 *modification during the calibration process, with the following exhibiting strong control on streamflow:*
1033 *SCS runoff curve number, Manning’s n value for the main channel, effective hydraulic conductivity of the*
1034 *channel, initial volume of groundwater, recharge delay time, fraction of deep aquifer percolation, and*
1035 *snowfall temperature (Wei et al., 2018). Further details regarding calibration, model implementation, and*
1036 *hydrologic results are found in Wei et al. (2018).”*

1037
1038
1039
1040
1041
1042
1043
1044
1045
1046
1047
1048
1049
1050
1051
1052
1053
1054
1055
1056
1057
1058
1059
1060
1061
1062
1063
1064
1065
1066
1067
1068
1069
1070
1071
1072
1073
1074
1075
1076
1077
1078
1079
1080
1081
1082
1083
1084

(3) Line 60-61,” The soil water and groundwater concentration of each salt ion is also affected by equilibrium chemistry reactions: precipitation-dissolution, complexation, and cation exchange”. Actually, the reactions also happen in the surface water, why not consider the chemical reactions in surface water?

Response: The reviewer has raised a valid point. However, due to the large flow and extremely high in-stream salt ion concentrations in the Arkansas River, the mass transfer of equilibrium chemistry reactions likely is negligible compared to the mass transported with advection. The application of the model to the Arkansas River Valley therefore does not depend on in-stream chemical processes. A future version of the modeling code may include in-stream equilibrium chemistry reactions.

(4) Line 294,” Only minimal manual calibration was applied to the model, to yield correct magnitudes of salt ion concentration in soil water, groundwater, and stream water. Targeted parameters were the solubility product of CaSO₄ precipitation-dissolution, and the soil fraction of CaSO₄.” Why is only the CaSO₄ used to calibrate the model? Is this due to the major ion is SO₄ in this region?

Response: Correct. These two parameters / model factors were used for calibration due to the predominance of SO₄ and Ca among the salt ions in the soil/groundwater system of the Arkansas River Valley. Reaction rates and fractions involving other salt ions do not have a significant effect on the total dissolved solids (TDS) in the river water. The following text has been added to clarify:

Lines 326-327:

“Due to the predominance of SO₄ and Ca among salt ions in the regional system, targeted parameters were the solubility product of CaSO₄ precipitation-dissolution, and the soil fraction of CaSO₄.”

(5) What are the principle for setting the HRU with 5270? In Line 225, “Initial concentrations are required for each HRU.” Were all the salt concentration of these 5270 HRU measured? Otherwise, how would you set the initial value?

Response: As discussed in Wei et al. (2018) and on Lines 266-267, each cultivated field was designated as a separate HRU. As explained on **Lines 315-316**, *“Initial salt ion concentrations in soil water and groundwater were based on averages of observed groundwater concentrations.”*

Results indicate, however, that the initial concentration values for the HRUs do not have a significant effect on model results (also see Figure 14):

Lines 234-236:

“However, as will be shown in Sect. 3, using uniform (i.e. all HRU values are the same) concentration values yields the same result as using spatially-variable initial concentrations, if a warm-up period of several years is used in the SWAT simulation.”

(6) Line 350. The simulations for TDS and SO₄ are much better than other ions, what are the possible reasons? Is this related to the targeted parameters of CaSO₄ been used in calibration mentioned in Line 294? So, if the model is used in other cases, how would you choose the targeted parameters in the calibration? How about choosing other targeted parameters in this case?

Response: Yes, the statistical measures of the simulated concentrations for SO₄ in groundwater are very close to the measures of the measured concentration values, although the comparison for the other ions is

also good. As mentioned by the reviewer, this may be due to the fact that the two targeted parameters (CaSO₄ solubility product; soil fraction of CaSO₄) have a significant control on resulting SO₄ concentration values in soil water, groundwater, and river water. Results for the other ions can be improved through modifying the soil salt mineral fractions (for CaCO₃, MgCO₃, and NaCl). During the revision process we ran model scenarios with varying soil salt mineral fractions for these three salt minerals, and indeed the in-stream concentrations of CO₃, Mg, Na, and Cl increased and were close in magnitude to the observed values. However, concentrations in the tributaries (Timpas Creek, Crooked Arroyo) were too high. We have summarized these new scenarios and results in Figure 7 and the following text:

Lines 351-361:

“The cause for the under-prediction of these ions may be due to the unobserved presence of MgSO₄, MgCO₃, and NaCl in the soil. These minerals are not observed in NRCS soil surveys of the region, and hence were not included in the baseline model. However, several model scenarios were run to investigate the influence of these minerals. Soil bulk fractions between 0.0001 and 0.0005 were applied for these three minerals, with a large resulting effect on in-stream concentrations of Mg, Na, Cl, and CO₃. For example, using a fraction of 0.0002 resulted in correct magnitude of these four ions at the Las Animas site, but over-estimated concentrations in the tributaries (e.g. Timpas Creek) (Figure 7). This model scenario, however, applied uniform salt mineral fractions of MgSO₄, MgCO₃, and NaCl across all 5270 HRUs. Applying spatially-varying fractions across the watershed could provide the correct magnitude of in-stream concentrations of all ions at all stream sampling sites. Regardless, measured in-stream concentrations can provide key information as to the salt minerals present in the watershed, and differences between model output and field data highlight the need for better field survey data of salt mineral content in soils.”

(7) As shown in Fig.5, the simulation results in Rocky Ford Site are much better than those in Crooked Arroyo Site. What are the reasons? The simulation results of Na, Mg should be also shown to judge the model accuracy since the relative high concentration of these two ions as shown in Table 2.

Response: Correct: the model performs better at the Rocky Ford Site as opposed to the Crooked Arroyo site. As discussed in the text, the Rocky Ford Site is along the Arkansas River (high flows, high salt loads) whereas Crooked Arroyo is a small tributary wherein the only loadings of salt occur through non-point sources (surface runoff, lateral flow, groundwater flow, with the majority of loading via groundwater flow). As such, it is not (at least to the authors, who are familiar with the study area) surprising that model results are not as accurate as for the main stem of the river. In fact, we are quite encouraged with the level of salt loading and in-stream salt ion concentrations that were achieved by the model, as small drainage tributaries in agricultural areas are notoriously difficult to model in terms of in-stream solute concentration. This is discussed in the text:

Lines 368-371:

“The relationship for Crooked Arroyo yields an R² value of 0.80. This is particularly promising given that there is no specified upstream loading for the tributaries, and hence all salt mass within the stream system is due to surface runoff, lateral flow, and groundwater discharge. Hence, comparing simulated and observed in-stream salinity concentration in these two systems is a strong test for the model.”

As to the second point, Na, Mg, K, and CO₃ were not included in the original manuscript due to space constraints and due to the low overall contribution of these ions to the total dissolved solids concentration (particularly in the case of K and CO₃, which have very low concentrations in both measured data and in the model output). However, all ions have now been included in Figure 5. The Timpas Creek and Las Animas sites have also been added to Figure 5. Please also notice that the time series charts in Figure 5

(and in other figures) show only 2006-2009, the time period beyond the warm-up period and during which there are measured data. This allows the reader to see more clearly the temporal fluctuations of the salt ion concentrations, and the comparison with the measured data.

(8) From Fig.5 and Fig.6, the simulated ion concentration fluctuated much stronger than the observed value, even the simulated value closed to zero. Is this caused by the numerical instability of coupling the ion reaction module with SWAT? Or what are the major factors resulting in the strong fluctuations?

Response: The reviewer has raised an important point. Upon further analysis, the strong fluctuations are due to the groundwater loading of salts to the river and tributaries during strong rainfall events (this can be seen by the groundwater salt loadings shown in Figure 13B, with the highest loading days coinciding with the “spikes” in the in-stream concentration plots in Figures 5 and 6). The reason for the enhanced fluctuations in the model, as compared to the measured data, is the simplistic manner in which SWAT simulates groundwater flow: with 1D steady-state flow equations rather than a physically-based, spatially-distributed method using the groundwater flow equation. This could be remedied by linking SWAT with a physically-based groundwater model such as MODFLOW, but also must include a groundwater reactive solute transport model such as RT3D.

The following text has been added to summarize this insight:

Lines 423-428:

“Notice that the highest groundwater loading rates coincide with the “spikes” in the in-stream concentration plots of Figures 5 and 6, indicating the strong influence of groundwater loading on in-stream salt concentrations. The fluctuations in simulated in-stream concentration, however, are larger than observed with the measured values. This is due to the manner in which SWAT simulates groundwater return flow, with a steady-state flow equation for each HRU that provides pulses of groundwater to streams rather than the multi-dimensional groundwater flow equation that provides physically-based, spatially-distributed diffuse flow through the aquifer towards the stream network.”

(9) More discussion about the contribution of different ions on salt accumulation should be added in the case discussion. Only the salt balance components for TDS were analyzed in Fig.12.

Response: We agree that a more in-depth ion-specific analysis would be helpful. However, currently the modeling code does not have the capability of outputting basin-wide salt balance information for each of the salt ions. This is due mostly to constraints on sizes of the text files, which would become inordinately large due to the detailed output for each salt ion, but also due to the fact that often a basin-wide mass balance is not performed for each salt ion, and hence the output data would not be useful. Rather, ion-specific model data are output for concentrations in soil water, groundwater, and stream water, since these values often have been measured in the field and thus are available for model testing. Later versions of the modeling code may include basin-wide mass balance components for each salt ion.

(10) Line 329-332, are the portions of salt load calculated by the model? How would you judge the reasonability of the results?

Response: Yes, the model output can be used to calculate the portions of salt load from each hydrologic pathway. Testing these values (from Figure 9) against field data is much more difficult than the direct testing/comparison of soil water concentration, groundwater concentration, and in-stream concentrations (as performed in Figures 5, 6, 7, 8, and 12). However, groundwater loadings are compared to a field

1181 estimate of mass loadings (Figure 10). Also, PERC (soil percolation) loadings are tested indirectly through
1182 the accuracy of the groundwater loadings, since groundwater salt loadings are driven in part by the amount
1183 of salt loaded to the aquifer via soil percolation.
1184

1185
1186
1187

1188 Minor revisions:

1189

1190 (1) Line 33, SO₄⁻, should be SO₄²⁻. All the ions should be shown with positive and negative charges in all
1191 the other parts in the manuscript.

1192 [Response](#): This has been changed on Line 33 and in the Abstract, Introduction, and Methods text. However,
1193 the charges have been omitted elsewhere due to our assumption that the reader is familiar with these
1194 common ions.

1195

1196

1197 (2) Line 88, “later”, should be “lateral”?

1198 [Response](#): Yes. This has been changed.

1199

1200

1201 (3) Line 133, “mas”, should be “mass”.

1202 [Response](#): This has been changed.

1203

1204

1205 (4) Line 176, “C and D are reactants.” Should be “C and D are products.”

1206 [Response](#): This has been changed.

1207

1208

1209 (5) Line 177, what is the equation of iA ?

1210 [Response](#): The equation is portrayed using text: “*is computed by multiplying the activity coefficient γ_i by*
1211 *the molal concentration*”

1212

1213

1214 (6) Line 180, “mi”, should be “mⁱ”.

1215 [Response](#): This has been changed.

1216

1217

1218 (7) Line 197, there is two “in” in the sentence

1219 [Response](#): This has been changed.

1220

1221

1222 (8) Line 250, “SO₄” should be “SO₄²⁻”

1223 [Response](#): We have changed this to “SO₄”, using the common notation throughout the manuscript.

1224

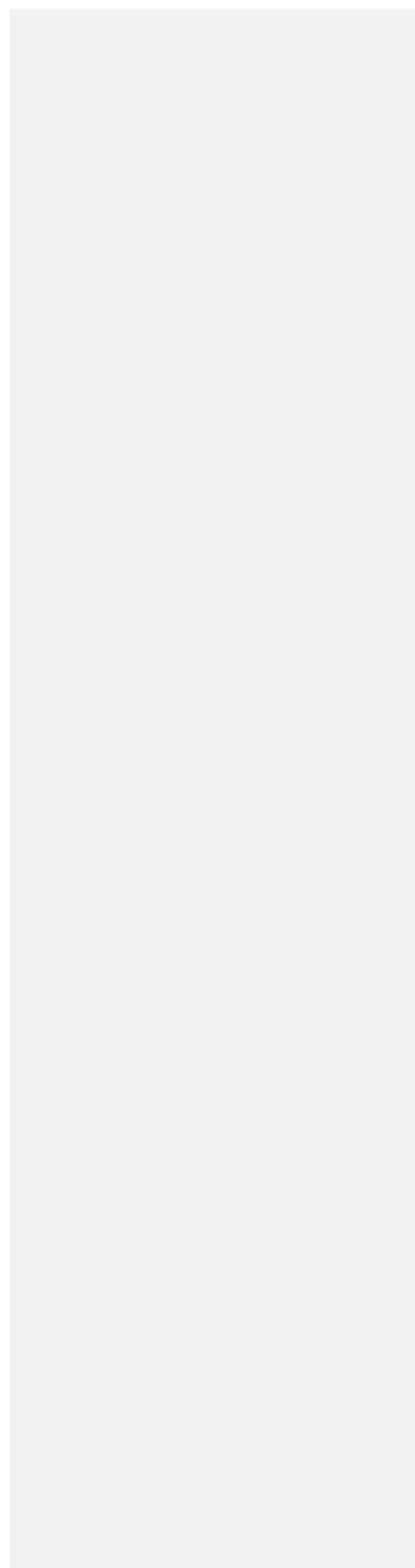
1225

1226 (9) Line 295, “produce” may be “product”?

1227 [Response](#): Yes. This has been changed.

1228

1229
1230 (10)Line 382, “mas” should be “mass”.
1231 [Response](#): Thank you. This has been changed.
1232
1233 **We thank Reviewer #1 for the helpful suggestions and comments.**
1234
1235
1236
1237
1238
1239
1240
1241
1242
1243
1244
1245
1246
1247
1248
1249
1250
1251
1252
1253
1254
1255
1256
1257
1258
1259
1260
1261
1262
1263
1264
1265
1266
1267
1268
1269
1270
1271
1272
1273
1274
1275
1276



1277 **RC2:**
1278 General comments: This work aims at simulating the fate and transport of 8 major salt ions (SO₄²⁻, Ca²⁺,
1279 Mg²⁺, Na⁺, K⁺, Cl⁻, CO₃²⁻, HCO₃⁻) in a watershed hydro-logic system using a new salinity transport
1280 module implemented in the SWAT code. This modelling code for salt transport includes surface runoff,
1281 percolation, soil lateral flow, groundwater flow and streamflow and also considers equilibrium chemistry
1282 reactions in soil layers and aquifers. This paper addresses with an interesting and practical approach the
1283 concerning thematic of soil and aquifer salinization. This study uses a quantification approach with salt
1284 balances performed in the watershed, includes the constituent mass in irrigation water, and the contribution
1285 of each salt ion to the salinity, which is less seen in published studies were the focus is the total of salts.
1286 Also, considering the new tool proposed that helps in predicting the impact of irrigation practices and in
1287 controlling salinity, I suggest the publication of this work after major revision.
1288 [We thank the reviewer for the comments.](#)

1289
1290 Specific comments:

1291
1292 1. Line 53 “Currently, there is no model that simulates salt trans-
1293 port in all major hydrologic pathways (surface runoff, soil percolation and leaching, groundwater flow, streamflow)
1294 at the watershed-scale that also considers important solution reaction chemistry.” Actually there is MOHID LAND
1295 model that is also coupled with SWAT. MOHID LAND is a physically-based, spatially distributed, continuous,
1296 variable time step model for the water and property cycles in inland waters and main mediums that also
1297 includes a chemical module PHREEQC that considers chemistry equilibrium of solution, pure phases, gas phase,
1298 solid phase, exchanges and surfaces in Porous Media (soil and aquifer). The authors should include in the
1299 Introduction section the existence of MOHID-LAND and make comparisons.

1300 [Response:](#) Thank you for the information. We were not aware of this model. However, we are not able to
1301 find any publications that describe the PHREEQC module for the MOHID modeling framework – we are
1302 only able to find a few references in on-line posts and a link to the source code. Also, the only reference to
1303 the linkage between SWAT and MOHID that we can find is a conference paper (“Integration of MOHID
1304 Model and Tools with SWAT Model”, from a 2007 SWAT conference). We would be happy to include a
1305 description of the linkage between SWAT and MOHID-PHREEQC, if the reviewer can provide references
1306 to published journal articles.

1307
1308
1309 2. There is some lack of detail on how the calculation routines for the new module are performed, namely
1310 how does it integrate salt ions reactions with the SWAT water flow and solute transport. How many
1311 parameters were used in the model calibration and validation? The data needed for SWAT modelling is not
1312 clear where it comes from, for e.g. the land cover, the soil, the crop and meteorological data (databases?).

1313 [Response:](#) We have added text to describe each of these points:

1314
1315 **Line 223-229:**
1316 *“The salinity chemistry reactions (precipitation-dissolution, complexation, cation exchange) are simulated*
1317 *for each HRU within the salt_chem subroutine (see Figure 2). Within the salt_chem subroutine, the*
1318 *chemistry reactions are applied to the current simulated concentration values of the 5 salt minerals and the*
1319 *8 salt ions for each soil layer and aquifer, to calculate new concentration values. These new concentration*
1320 *values are then used to simulate salt leaching (salt_lch subroutine) and salt ion loading in surface runoff*
1321 *(surfstor) and groundwater flow (salt_gw, substor) (Figure 2). At the end of each daily time step, the*
1322 *simulated salt ion mass (kg) in each transport pathway (irrigation, leaching, runoff, percolation, lateral*
1323 *flow, groundwater flow, dissolution/precipitation) is stored for mass balance assessment and output.”*
1324

1325
1326
1327
1328
1329
1330
1331
1332
1333
1334
1335
1336
1337
1338
1339
1340
1341
1342
1343
1344
1345
1346
1347
1348
1349
1350
1351
1352
1353
1354
1355
1356
1357
1358
1359
1360
1361
1362
1363
1364
1365
1366
1367
1368
1369
1370
1371

Lines 282-283:

“The digital elevation model (DEM), stream network, soil map, land-use map, climate data, streamflow, and canal diversion data were obtained from the USGS, NRCS, and several state agencies, as summarized in Wei et al. (2018).”

Lines 293-298:

“Calibration was performed using SWAT-CUP (Abbaspour et al., 2008) using the observed streamflow at the Rocky Ford, Las Animas, and Timpas Creek stations. Twenty parameters were targeted for modification during the calibration process, with the following exhibiting strong control on streamflow: SCS runoff curve number, Manning’s n value for the main channel, effective hydraulic conductivity of the channel, initial volume of groundwater, recharge delay time, fraction of deep aquifer percolation, and snowfall temperature (Wei et al., 2018). Further details regarding calibration, model implementation, and hydrologic results are found in Wei et al. (2018).”

3. For each HRU the mass of the several salt ions is generated by the several processes. In runoff how is defined the salinity percolation coefficient ($\tau_{A c Si}$) and the surface runoff lag coefficient (surlag), what value is attributed and why? Explanation is needed.

Response: The concentration of salinity in surface runoff is determined by the salinity percolation coefficient (0 to 1), which in this model is assumed to be the same as the nitrate percolation coefficient (= 0.2). Therefore, surface runoff salinity concentration is 20% of the concentration value of the salinity in percolate water. The surface runoff lag coefficient is 2.0 days, and was not adjusted for any HRU during calibration of the salinity model. This value was determined during the calibration of the hydrologic model in Wei et al. (2018).

4. Line 144-145, “The mass of each salt ion is routed through the channel network with water, with no chemical reactions changing in-stream salt ion concentration”. Why no chemical reactions are considered in-stream to change salt ion concentration? Chemical reactions also happen in in-stream water, right?

Response: The reviewer has raised a valid point. However, due to the large flow and extremely high in-stream salt ion concentrations in the Arkansas River, the mass transfer of equilibrium chemistry reactions likely is negligible compared to the mass transported with advection. The application of the model to the Arkansas River Valley therefore does not depend on in-stream chemical processes. A future version of the modeling code may include in-stream equilibrium chemistry reactions.

5. Line 225, “Initial concentrations are required for each HRU.” And Line 226-227 authors refer that “...(all HRU values are the same) concentration values yields the same result as using spatially-variable initial concentrations, if a warm-up period of several years is used in the SWAT simulation.” Why it was not considered the average concentration for each sampling site spatially located near the HRU? From a theoretical point of view, does not seem correct to use as inputs non-spatially concentrations, even because the model will need a warm-up period of several years.

Response: Certainly spatially-dependent values of soil and groundwater salt ion concentrations can be used to initialize HRU values, and therefore be more accurate at the onset of the model simulation period. We assumed that this would be necessary. However, during scenario testing it was observed that the model results, at least for this study region, are not significantly sensitive to initial conditions, given several years

of warm-up. This is the point of the scenario and associated conclusion, which is presented in Section 3.3.2.4 (“Scenarios and Model Guidelines”):

Lines 440-442:

“There are only small differences between using uniform or HRU-variable initial concentrations for soil water and groundwater. Any differences are readily resolved during the warm-up period. Hence, to facilitate model use we recommend that uniform initial concentrations be used.”

6. Line 297-299, “Observed soil EC values were obtained using a saturated paste extract, and hence comparison with model results will not be as rigorous as for groundwater and surface water data.” Why the comparisons with model results will not be as rigorous as for groundwater and surface water data? EC measured in a saturated paste extract (EC_e) is related to the EC of the soil water (EC_{sw}). Have you considered to use of Ayers and Westcot (1985) conversion, Skaggs et al. 2006 or using other conversion with the % saturation?

Response: Thank you for commenting on this. We agree that we should compare estimated field-measured EC of soil paste extract with estimated simulated values. This was performed during the revision process by converting soil water TDS to EC_w, and then to EC_e using the ratio of soil water (mm) to water amount at saturation (mm) for the SWAT soil layers. This was performed for all cultivated HRUs during the 2002-2005 growing season, coinciding with the period of field sampling. The SWAT code was modified to output these data. The results are shown in Figure 12D (revised manuscript) using frequency distributions of the observed and simulated values. The following text was added to describe the field surveys and then provide analysis of results:

Lines 272-278:

“Average soil water salinity, based on electrical conductivity of a soil paste extract (EC_e), is 4.11 dS/m (54700 measurements), with minimum and maximum of 0.9 dS/m and 56.5 dS/m, respectively (Morway and Gates, 2012). These values were estimated from measurements of apparent bulk soil conductivity, taken with a Geonics EM-38 electromagnetic induction sensor, as described in Morway and Gates (2012). Surveys were performed during the months of March-September for 1999-2005. Based on 6 surface water sampling sites (4 in the Arkansas River, 2 in tributaries; Figure 3B), average C_{TDS} and C_{so4} is 1145 mg/L and 560 mg/L, respectively. More details of observed groundwater, soil water, and surface water concentrations are provided in Sect. 3.3.2 when model results are presented.”

Lines 402-411:

“A relative frequency plot of observed and simulated EC_e (dS/m) in the soil profile is shown in Figure 12D. The simulated values were taken from HRUs coinciding with cultivated fields for the days of April 15, May 15, June 15, July 15, and August 15, for the years 2001-2005. Note that simulated values were taken from each cultivated HRU, whereas the field surveys using the EM-38 sensors were conducted in approximately 100 fields. The average of observed values is 4.1 dS/m, although this number is skewed by extremely high values (> 30 dS/m). If only values < 6.5 dS/m are considered (89% of the samples), then the average is 3.2 dS/m. The average of the simulated values is 2.96 dS/m. As seen from the frequency distribution in Figure 12D, the model tends to under-estimate soil salinity for some of the HRUs, and does not capture the high salinity values (> 7 dS/m). However, the overall magnitude and distribution of values approaches the distribution of the measured values. Note that EM-38 measurements have inherent uncertainty. In addition,

1419 *some of the HRUs included in the analysis are fallow during this period (2002-2005), which may lead to*
1420 *low soil salinity values that were not measured in the field survey.”*

1423 7. Line 293-294, “Only minimal manual calibration was applied to the model, to yield correct magnitudes
1424 of salt ion concentration in soil water, groundwater, and stream water.” Why this approach of minimal
1425 manual calibration? And why just consider SO₄²⁻ for calibration? Even understanding that from your
1426 sampling the SO₄ accounted for 47% of total in-stream salt mass, it would be a more solid calibration using
1427 other salt ions (especially Na), and more applicable to other studies. Can you calibrate with more salt ions?

1428 **Response:** The word “minimal” was used to indicate that only two parameters were varied during model
1429 calibration. We changed the wording to read:

1431 **Lines 325-327:**

1432 *“Manual calibration was applied to the model to yield correct magnitudes of salt ion concentration in soil*
1433 *water, groundwater, and stream water. Due to the predominance of SO₄ and Ca among salt ions in the*
1434 *regional system, targeted parameters were the solubility product of CaSO₄ precipitation-dissolution and*
1435 *the soil fraction of CaSO₄.”*

1437 However, to the reviewer’s point, parameters governing the other salt minerals (CaCO₃, MgCO₃, and
1438 MgSO₄) could be varied to provide a better match between observed and simulated salt ion concentrations
1439 in the groundwater and river water. We tested this during the revision process, running model scenarios
1440 with varying soil fractions of these three salt minerals. Indeed, the in-stream concentrations of CO₃, Mg,
1441 Na, and Cl increased and were close in magnitude to the observed values. However, concentrations in the
1442 tributaries (Timpas Creek, Crooked Arroyo) were too high. Therefore, perhaps unobserved fractions of
1443 these salt minerals may be present in the watershed soils. We have summarized these new scenarios and
1444 results in Figure 7 and the following text:

1446 **Lines 351-361:**

1447 *“The cause for the under-prediction of these ions may be due to the unobserved presence of MgSO₄,*
1448 *MgCO₃, and NaCl in the soil. These minerals are not observed in NRCS soil surveys of the region, and*
1449 *hence were not included in the baseline model. However, several model scenarios were run to investigate*
1450 *the influence of these minerals. Soil bulk fractions between 0.0001 and 0.0005 were applied for these three*
1451 *minerals, with a large resulting effect on in-stream concentrations of Mg, Na, Cl, and CO₃. For example,*
1452 *using a fraction of 0.0002 resulted in correct magnitude of these four ions at the Las Animas site, but over-*
1453 *estimated concentrations in the tributaries (e.g. Timpas Creek) (Figure 7). This model scenario, however,*
1454 *applied uniform salt mineral fractions of MgSO₄, MgCO₃, and NaCl across all 5270 HRUs. Applying*
1455 *spatially-varying fractions across the watershed could provide the correct magnitude of in-stream*
1456 *concentrations of all ions at all stream sampling sites. Regardless, measured in-stream concentrations can*
1457 *provide key information as to the salt minerals present in the watershed, and differences between model*
1458 *output and field data highlight the need for better field survey data of salt mineral content in soils.”*

1461 8. Line 314, “The model does not perform as well in downstream sites, with NSE at La Junta and at Las
1462 Animas”. Why the model performance is better in Rocky Ford site than in Crooked Arroyo site? What are
1463 the reasons for the weaker performance at downstream locations? Explain better in the manuscript.

1464 **Response:** Likely, the model performs better at the Rocky Ford site due to the proximity to the upstream
1465 end of the watershed, where loading for each salt ion is specified for each day. However, through visual
1466 inspection (Figure 6), the model performs adequately in simulating the temporal fluctuation and magnitude

1467 of TDS at the La Junta gage, with only one measured concentration value, from January 17, 2009, much
1468 different than the simulated value – this is actually due to an over-estimation of streamflow by SWAT, and
1469 thereby an under-prediction of in-river concentration.
1470

1471 However, during the revision process we noticed that we were using an old version of the SWAT model,
1472 which over-estimated flow in the downstream reaches of the watershed, and thus under-estimate the in-
1473 stream salt ion concentrations. Using the most up-to-date version of the model (as seen in Wei et al., 2018),
1474 the downstream flows match the observed flows much more closely, and hence the simulated in-stream salt
1475 ion concentrations are much closer in magnitude to the measured values. This can be seen in Figure 5D and
1476 Figure 6E for the Las Animas site.
1477
1478

1479 9. In Fig. 14 it is observed the importance of including equilibrium chemistry into the salt transport. The no
1480 SEC simulations are underestimating the in-stream TDS. Can you explain why this underestimation is not
1481 so evident in the downstream location Las Animas? I was not expecting this.

1482 [Response](#): This effect at Las Animas was due to the use of the outdated SWAT model, which overestimated
1483 flow in the downstream reaches of the Arkansas River (see response to previous comment). Using the up-
1484 to-date SWAT model, the results for the Las Animas site (Figure 15C) (i.e. under-predicting in the scenario
1485 of no SEC) are similar to other sites. However, notice that the results for the Rocky Ford site (Figure 15A)
1486 show only small differences between the scenarios. For the Rocky Ford site, the scenarios yield similar
1487 results due to the location of the site being close to the upstream end of the modeled region, and thus in-
1488 stream concentrations are not affected by groundwater and surface runoff salt loadings to the river (Lines
1489 464-466).
1490

1491
1492 Technical corrections:
1493

1494 1. All ionic forms must be written considering the ionic charges (e.g. SO_4^{2-} , HCO_3^- , etc.). Correct in all the
1495 manuscript.

1496 [Response](#): The charges are included in Table 1 and in the Introduction and Methods text, but omitted
1497 elsewhere due to our assumption that the reader is familiar with these common ions.
1498

1499 2. Line 59,79, 88: where it is written “soil later flow” should be “soil lateral flow”?

1500 [Response](#): This has been changed.
1501

1502
1503 3. Line 123: it is written “TTlag” should it be “TTlat”?

1504 [Response](#): Yes. This has been changed.
1505

1506
1507 4. Line 128: where the variable $Q_{lat,ly}$ is described, it should refer to $Q_{perc,ly}$.

1508 [Response](#): Thank you. This has been changed.
1509

1510
1511 5. Line 162: refer to the 8 aqueous species writing them in the ionic form.

1512 [Response](#): This has been changed.
1513
1514

1515
1516 6. Line 180: the molality is missing the subscript (mi).
1517 [Response: This has been changed.](#)
1518
1519
1520 7. Line 191: the equation mentions NaCO₃-that differs from the complexed specie NaCO₃ in table 1.
1521 Correction needed.
1522 [Response: This has been corrected.](#)
1523
1524
1525 8. Line 197: there are two “in” in the sentence.
1526 [Response: This has been changed.](#)
1527
1528
1529 9. Line 176: C and D should be the products.
1530 [Response: This has been changed.](#)
1531
1532
1533 10. Line 177: Present the equation for it
1534 [Response: This is provided using text.](#)
1535
1536
1537 11. Line 216: It is written “(meq/100)” and it should be “(meq/100g)”.
1538 [Response: This has been changed.](#)
1539
1540
1541 12. Line 246: The use of commas in separation of group numbers was confusing when referring to
1542 concentrations of mg/L. In HESS guidelines for authors states that “Neither dots nor commas are permitted
1543 as group separators.” Correct this in all manuscript.
1544 [Response: Thank you. Commas have been removed from numbers throughout the manuscript.](#)
1545
1546
1547 13. Line 318: The sentence “Las Animas also has an R² value of 0.74.” appears redundant since the R² was
1548 already commented in the previous sentence. Did the authors wanted to comment the R² for Timpas Creek?
1549 [Response: Yes. This has been changed.](#)
1550
1551 14. Line 324: “The relationship for Crooked Arroyo yields an R² value of 0.80.” This refers to data not
1552 shown?
1553 [Response: Yes. This has been changed in the text.](#)
1554
1555 15. Line 334: There are to “a” before stochastic in the sentence.
1556 [Response: Thank you. This has been corrected.](#)
1557
1558 16. Line 382: its written “mas” and should be “mass”.
1559 [Response: This has been changed.](#)
1560
1561 **We thank Reviewer #2 for the helpful suggestions and comments.**
1562

1563 **EC1:**
1564 L: 217: Generally, the cation exchange capacity is pH-dependent. Is this taken into account by the model?
1565 If not, what are the reasons?

1566 Response: pH was not simulated in the model. The salinity module used in SWAT-Salt is based on
1567 Tavakoli-Kivi et al. (2019: “A salinity reactive transport and equilibrium chemistry model for regional-
1568 scale agricultural groundwater systems. Journal of Hydrology 572, 274-293”), which does not account for
1569 pH. The module was not changed in this sense for imbedding within SWAT. In addition, the precipitation-
1570 dissolution reactions dwarf the cation exchange process in terms of governing salt ion concentration, and
1571 hence we believe that the exclusion of pH dependency is not critical for this study region. It will be re-
1572 visited for future studies and model applications.
1573
1574

1575 L: 293 - 295: You mention that only minimal manual calibration was applied. However, changing the
1576 solubility product by almost a one order of magnitude seems more than minimal. Can you provide reasons
1577 why it may be necessary to modify a solubility product?

1578 Response: The word “minimal” in the text refers to the low number (2) of parameters modified during
1579 manual calibration. This has been changed in the text:
1580

1581 **Lines 325-327:**

1582 *“Manual calibration was applied to the model to yield correct magnitudes of salt ion concentration in soil*
1583 *water, groundwater, and stream water. Due to the predominance of SO_4 and Ca among salt ions in the*
1584 *regional system, targeted parameters were the solubility product of $CaSO_4$ precipitation-dissolution and*
1585 *the soil fraction of $CaSO_4$.”*
1586

1587 Similar to groundwater salinity models that employ equilibrium chemistry, simulations indicate that model
1588 results are strongly dependent on the solubility product of the salt minerals. These solubility products are
1589 governed principally by temperature and pH. As temperature in the soil profile and aquifer differ, and also
1590 vary seasonally, and since pH is not modeled in the current model version, the solubility product of $CaSO_4$
1591 was modified during the calibration process since the true solubility product value is not known with
1592 certainty. However, the same value was used for both the soil profile and aquifer, with the value held
1593 constant for all HRUs.
1594
1595

1596 L: 334: What’s a stochastic river mass balance?

1597 Response: This refers to a salinity mass balance of the Arkansas River system, . For clarity, we have
1598 changed the text to the following:
1599

1600 **Lines 381-384:**

1601 “Mass balance plot values are the mean of an ensemble of a stochastic river mass balance calculation of
1602 surface water salinity loadings along the length of the Arkansas River within the model domain, using a
1603 method similar to Mueller-Price and Gates (2008), with values indicating the mass of salt not accounted for
1604 by surface water loadings.
1605

1606 Fig. 4A: In this figure one cannot distinguish the different ions. Please modify.

1607 Response: This figure was changed to show average daily salt ion loading, for each year (1999-2009). The
1608 values for each salt ion can now be seen more clearly.
1609

1610 **We thank the Editor for the helpful suggestions and comments.**